Fisheries New Zealand
Tini a Tangaroa

Assessment of risk factors for seabird net captures in selected sub-Antarctic trawl fisheries

New Zealand Aquatic Environment and Biodiversity Report No. 266

C.T.T. Edwards,
A. Dunn

ISSN 1179-6480 (online)
ISBN 978-1-99-100972-2 (online)

August 2021

New Zealand Government

Requests for further copies should be directed to:

Publications Logistics Officer
Ministry for Primary Industries
PO Box 2526
WELLINGTON 6140

Email: brand@mpi.govt.nz
Telephone: 0800 00 83 33
Facsimile: 04-894 0300

This publication is also available on the Ministry for Primary Industries websites at:
http://www.mpi.govt.nz/news-and-resources/publications
and http://fs.fish.govt.nz (go to Document library/Research reports)

TABLE OF CONTENTS

EXECUTIVE SUMMARY

Edwards, C.T.T.; Dunn, A. (2021). Assessment of risk factors for seabird net captures in selected sub-Antarctic trawl fisheries.

New Zealand Aquatic Environment and Biodiversity Report No. 266. **51 p.**

Mitigation measures introduced into New Zealand's trawl fisheries have significantly reduced the incidence of pelagic seabird captures. However, captures still occur, most predominantly by the net during hauling as birds attempt to feed through the net. Characterisation of the seabird bycatch indicates that net captures in the squid and middle-depth trawl fisheries, and in particular in the sub-Antarctic regions of New Zealand, account for the majority of captures. The current work is an attempt to assess possible contributory factors, and hence inform future management and further mitigation efforts.

To assess the risk factors associated with seabird captures in the sub-Antarctic trawl fisheries we developed a hierarchical model that describes the capture process as a function of selected covariates, including the target fishery, location (grid), season and vessel class. The model can accommodate multiple capture types using a multinomial observation process, making use of all the observational data. Including a management or behavioural covariate allowed us to construct a risk-based metric as a function of the estimated covariate value. Risk was defined as proportional to the probability of bird capture, across all capture types, and through comparison across covariate levels we were able to determine the relative risk associated with different fishing practices.

Covariates were used for the analysis that allowed us to investigate the contributions of the net configuration, weather conditions, time of haul during the day or night, moon phase, time of net on the surface during hauling and the local commercial fishing effort. We were able to identify instances in which fishing practices influenced the probability of bird capture, but the effect size of these covariates was small, with the capture probability typically ranging between 1% and 3%. Most notably, time of the net on the surface and the amount of other commercial fishing effort in the local vicinity had the strongest effect.

The modelling framework we developed was integrated over multiple observation categories, including different species groups, accommodated for missing covariate values, and allowed for a risk metric to be constructed directly as a function of model covariates. The risk is relative to the overall probability of bird capture. This makes it independent of information on the bird population size — a notable advantage over previously used risk assessment frameworks that require information on both the population size and distribution. The framework may therefore also prove useful in contexts that require assessment of the risk of fishing to other marine fauna.

1. INTRODUCTION

In New Zealand domestic fisheries, seabirds are caught during trawling operations and typically killed or injured through contact with either the trawl warps or the fishing net. The entanglement in the trawl net generally occurs when the net is close to or at the surface during haul time, as birds attempt to access food through the mesh. Seabirds can then be trapped in the meshes and sustain injuries or death. After the introduction of mitigation measures and vessel management plans on offal and setting procedures the number of seabirds reported as caught from warp strikes decreased. Although the number of bird injuries and deaths from net captures is relatively low compared with historical numbers of warp strikes, the numbers of net related injuries and deaths have remained constant or even slightly increased in recent years.

Observers for the Ministry for Primary Industries (MPI) who are present on some fishing vessels record captures of seabirds. These observer data provide a basis for evaluating the risk factors that influence the rate of seabird net captures on vessels and can inform development of potential mitigation strategies. Analyses of these data show that mitigation measures introduced in the 2005/06 fishing year substantially reduced the number of birds killed or injured from contacting the trawl warps and as a result total numbers of reported bird captures substantially declined (Baird & Doonan 2016). The observer data on seabird captures have previously been presented in a series of summary reports (e.g., Baird 2008, Abraham et al. 2016).

The most recent previous work (Baird & Doonan 2016) described the frequency and characteristics of seabird captures in the domestic offshore trawl fisheries around New Zealand using MPI Observer data from the MPI Centralised Observer Database (COD). They summarised the captures according to the broad seabird groups of Richard & Abraham (2015):

1. MED: for medium-sized seabirds (mainly shearwater and petrel taxa);
2. SALB: for small albatross taxa and giant petrels;
3. LALB: for large albatross taxa; and
4. SML: for small seabirds (mainly cape petrels, diving petrels, and storm petrels).

The characterisation by Baird & Doonan (2016) considered observer data from 2007/08–2014/15, covering the period after the introduction of new observer data collection forms in the mid-2000s. These forms recorded better information on the capture of protected species and were introduced after the widespread adoption of bird capture mitigation measures in these fisheries.

Baird & Doonan (2016) reported that a total of 3770 seabird captures were recorded between 2007/08 and 2014/15, of which 2732 were caught in the net (74%). Of these, 1990 (73%) were in the MED group, 690 (25%) in SALB, 40 (2%) in SML and 12 (less than 1%) in LALB. The MED and SALB species groups were therefore the most frequently caught.

Squid target trawl fisheries accounted for 64% of the MED net captures during 2007/08–2014/15, with over 100 seabirds reported in most years (except 2009/10–2011/12), and more than 300 MED seabirds during 2012/13 and 2014/15. Hoki target trawls accounted for another 12.5% of the MED net captures. SALB net captures were also mainly from squid (49%) and hoki trawls (24%).

Spatially, captures of both MED and SALB species were concentrated along the Stewart-Snares shelf in the Fishery Management Area FMA 5, and around the Auckland Islands (FMA 6 SOI), with some captures to the western end of the Chatham Rise (FMA 3) as well as its northern boundary (FMA 4).

Almost all (98%) MED net captures were reported between October and May, with most reported from February to April during the southern squid trawl fishery in FMA 5 and FMA 6 (Statistical Areas 027, 028, and 602). MED net captures from hoki trawls from October to May were mainly from FMA 3 on the western Chatham Rise. Squid target effort between January and July resulted in most SALB captures (Statistical Areas 028 and 602). SALB were also caught by middle-depth fisheries, especially hoki, during October–September across the Chatham Rise.

The characterisation by Baird & Doonan (2016) identified several factors associated with the capture of seabirds, primarily the spatial and temporal distribution of specific target trawl fisheries that overlap with the spatial and temporal distribution of the seabirds being caught. Other factors described in the report were the type of fishing (midwater versus bottom trawl), the presence of mitigation methods (designed to avoid warp strikes), and time of day for the haul. Insufficient data were available for their analyses to determine if the capture occurred during the shooting or hauling of the net. Similarly, it was difficult from the observer records analysed to discern patterns in how (i.e., what part of the net) birds were generally caught.

The current work builds upon the characterisation of Baird & Doonan (2016) by constructing a modelling framework to formally evaluate the risk factors that may contribute to bird captures. It extends the period of analysis to include fishing years from 2007/08 to 2017/18 and is restricted to those fisheries where the most captures have been recorded, specifically the squid (SQU) and the main middle-depth trawl fisheries (e.g., Hoki, Hake and Ling; HHL) operating in Statistical Areas 025–030, 504, 602, and 603 (FMA 5 and FMA 6 SOI).

The project objective was to assess risk factors that influence the rate of seabird net captures on larger trawl vessels to inform the development of potential mitigation strategies; with specific objectives (1) complete modelling analyses to examine the influence of factors that could potentially lead to the net captures of seabirds on large trawl vessels, and (2) based on the outcome of Objective 1, summarise and present potential mitigation strategies and a means to test these at a workshop.

2. METHODOLOGY

Formal assessment of the risks associated with different fishing practices is required for the development of mitigation measures with the potential to promote the conservation of bycaught species. Risk can be quantified in a variety of ways. For example, in the Potential Biological Removals (PBR) methodology (Hobday et al. 2011) risk was measured as the number of deaths over the number of deaths that the population can sustain. This was the approach adopted by the Spatially Explicit Fisheries Risk Assessment approach (SEFRA, Fisheries New Zealand 2020) used for seabird risk assessments in New Zealand (e.g., Richard et al. 2020). However, it is possible to measure *relative* risk without necessarily quantifying the total number of captures or deaths. For example, in medical science, an estimate of the risk of infection by a pathogen can be obtained without knowing how prevalent a particular disease already is. This interprets risk as the probability of occurrence. This is an easier and more robust approach, since all we require are data on the sampling effort and records of each incidence. In the current setting we are concerned with bird captures, and we propose to measure risk as the probability that a bird capture takes place. We can calculate this probability using observed fishing effort, since both the sampling effort and incidence are known (assuming all captures in the observed trawls were recorded).

The different approaches to quantification of the risk also require different emphases. For SEFRA,

the emphasis is on developing an absolute estimate of the total number of deaths. This is a difficult estimation problem because most of the deaths will not be observed, usually because there is no observer on the vessel or because a tow may not be observed even when the observer is on the vessel. However, if we consider a relative measure of the risk then we only need to use the observed fishing effort. Here, the most important consideration is not the total number of captures but the observed effort per recorded capture. In addition, with the seabird capture data, there can be multiple capture observations per unit of effort. For example, more than one bird species or more than one bird of a specific species may be caught on a single tow. To measure risk therefore, we need to estimate the probability of bird capture whilst simultaneously considering multiple captures across multiple observation categories.

An appropriate statistical model for this type of data can be implemented using a conditional multinomial (MNL) observation process. If observers record captures per fishing event, with these captures being assigned to one or more discrete categories, then when more than one capture is observed then the outcome per tow can described using a multinomial probability distribution:

$$\{y_{i1},\ldots,y_{ik}\} \sim MNL(n_i,\pi_1,\ldots,\pi_k) \quad \text{for} \quad n_i > 0 \tag{1}$$

where $n_i = \sum y_{ik}$ is the number of captures per fishing event i, and $\sum \pi_k = 1$ are the probabilities per observation category k. The different observation categories may include species, type of capture and whether the bird is alive or dead. Because the number of captures per tow is itself a random variable, it also has a probability distribution. In this case, we assume a Poisson distribution (i.e, that the probability of a capture occurring during a specific interval of time is constant and each capture is independent of all other captures):

$$n_i \sim P(\lambda \cdot E) \tag{2}$$

which allows for zero-capture observations, i.e., $n \geq 0$. Given the effort E, our intention is to estimate the rate parameter λ, from which we can calculate the probability of there being at least one bird capture for any given tow:

$$\text{Risk} = \mathbb{P}[n_i > 0|\lambda] \tag{3}$$

This is the approach adopted for the current assessment, in which we attempt to estimate the relative risk associated with different fishing practices or management measures. We note that it represents a generic risk assessment framework for situations where the absolute number of deaths is difficult or not possible to quantify, but where we have accurate data on the numbers of deaths for each observed tow.

3. DATA PREPARATION

Data from the protected species capture database were obtained directly from Fisheries New Zealand and consisted of three tables: 1) observer reported captures; 2) observer recorded fishing effort; and 3) commercial fishing effort. A series of standard grooming procedures were applied that included checking and either deleting or correcting (where plausible numbers were able to be discerned) the observations. These included:

- Consistency of time and date fields — ensuring end time was always after the start time, assuming end time was incorrect for excessively long tows and the imputation of missing duration data;

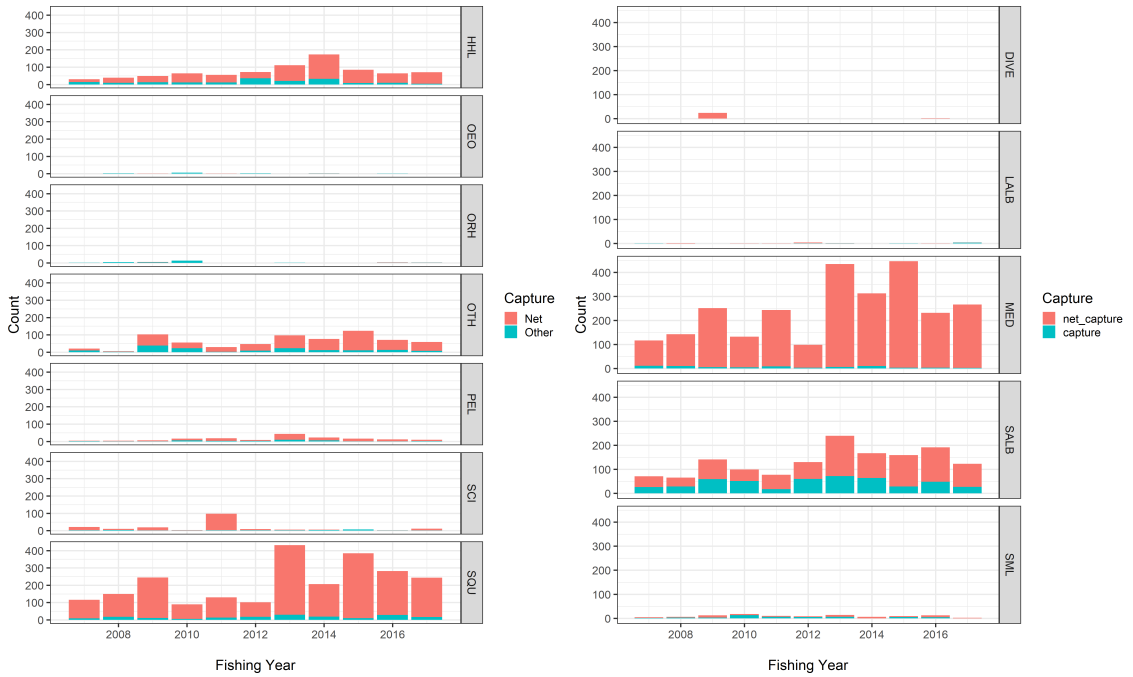

Figure 1: Number of seabird captures by fishing year, target fishery, and species group (MED: medium-sized seabirds; SALB: small albatross taxa and giant petrels; LALB: large albatross taxa; and SML: small seabirds) for net and other captures.

- Position of tows — with the deletion of the end point for zero length or excessively long tows, imputation of missing distance values and the removal of tows with no start position coordinates, on land or outside of the EEZ.

The raw capture data are given in Appendix A. Consistent with Baird & Doonan (2016), the majority of captures were of the SALB and MED species groups (Table A1), and by trawl nets in the HHL and SQU fisheries (Tables A2, A3, and A4), operating around the Auckland Islands and Stewart-Snares shelf (Table A5). Species groups (Appendix B) were identical to those used by Baird & Doonan (2016), albeit with with minor modifications in consultation with Fisheries New Zealand. This included the definition of an additional species group (diving seabirds) — however, there were no birds from this category in the data analysed here.

Total captures per fishery, extracted from the raw data, are shown in Figure 1. Only trawl data from vessels greater than 42 m in length from the squid (SQU) and middle-depth (HHL) fisheries and from the 2007/08 fishing year onward were retained. Data were further constrained to Statistical Areas 025 – 030, 504, 602 and 603, and each tow was assigned spatially to a grid of 0.2° by 0.2°. The data were restricted to those areas and target species where there had been consistent observations over time, while also including as much data as possible to allow robust estimates of risk. This data subset is shown in Table 1. For these data, the number of observed trawl captures and the capture rate over time are also shown in Figure 2, with captures in other regions shown for comparative purposes.

In addition to the data from the protected species capture database, Fisheries New Zealand provided information on the waste management strategy adopted by each vessel (as recommended for further analysis by Baird & Doonan 2016), the configuration of the net on each tow (including the mesh sizes and the type of mesh used in various parts of the net), the weather at the time of each tow, and time that the net remained on the surface during the haul.

Table 1: Model data subset. For the whole of New Zealand, there were a total of 2,380 captures out of 17,740 observed tows in the SQU fishery; and 1,098 captures out of 39,965 observed tows in in the HHL fishery.

Fishing Year	SQU			HHL		
	Total effort	Observed effort	Captures	Total effort	Observed effort	Captures
2006/2007	6 497	1 242	106	1 079	418	5
2007/2008	7 842	1 450	150	1 674	694	9
2008/2009	6 938	1 280	245	986	612	11
2009/2010	5 092	1 063	89	1 581	760	20
2010/2011	6 061	1 242	129	845	509	28
2011/2012	4 783	1 358	102	954	544	28
2012/2013	8 014	2 238	429	2 124	1 094	36
2013/2014	6 275	1 778	205	1 408	857	51
2014/2015	5 369	1 624	382	1 426	691	30
2015/2016	10 425	2 124	258	987	554	20
2016/2017	7 893	1 812	243	863	448	20
Total	75 189	17 211	2 338	13 927	7 181	258

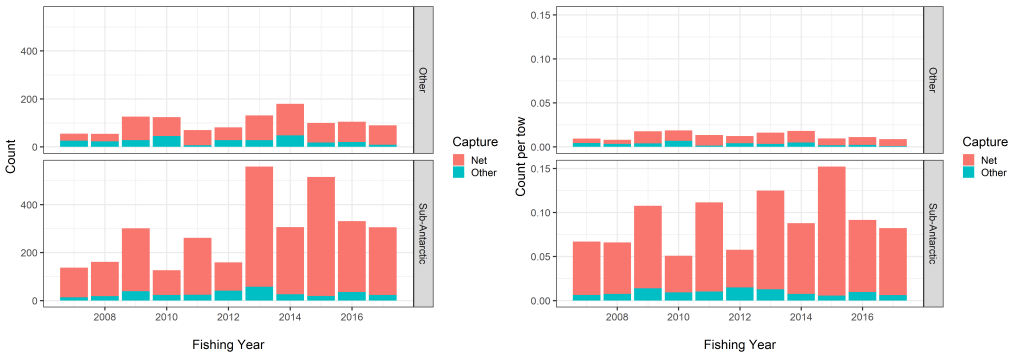

Figure 2: Number of observed seabird captures and seabird capture rate by fishing year for the squid (SQU) and hoki, hake, and ling (HHL) trawl fisheries, with the "Sub-Antarctic" defined for the purposes of the current study as Statistical Areas 025, 026, 027, 028, 029, 030, 504, 602, 603.

Haul times and positions were taken to be the end points recorded in the observer data, except where these were missing or marked during the grooming procedure as erroneous. In these cases the start times and positions were used instead. The data were then combined using the following steps:

- Captures were joined to the observer data using the "station_number" and "trip_number" fields in the database and using the capture identification field "cid" to ensure no duplication of captures (note that this duplicates the effort in cases where more than one capture was recorded for a given record); where the start and end positions were different, the observer data were assumed to be more accurate;
- Commercial effort data were joined to the observer data using the "event_key" field;
- Waste management strategy data were joined to the observer data using the "vessel_key";
- Data on the gear configuration, weather (Beaufort scale) and net time on the surface were joined to the observer data using the "station_number" and "trip_number" fields;
- Commercial trawl effort summed by grid, year and calendar day was assigned as a covariate.

Hence, we modelled seabird captures by their species group, season, capture type, and location

(grid) using the following covariates (chosen in consultation with Fisheries New Zealand as likely to be the most relevant to captures) for all years since 2007/08:

- Mesh configuration (Diamond, Hexagonal, Square, or Rotated for the lengthener and codend);
- Gear configuration (sweep length, headline height, headline length, lengthener mesh size, and codend mesh size);
- Vessel characteristics, specifically the length, gear configuration and waste management practices (Meal, Batch, or Mince);
- Moon phase;
- Capture hour, alternatively expressed as the circadian time (specifically whether the haul occurred during the dawn, day, dusk, or night) whilst accommodating changes in the time of sunrise and sunset with season;
- Commercial trawl fishing effort in local vicinity (i.e. within the same 0.2° by 0.2° grid);
- Time of net on surface during haul;
- Weather (measured using the Beaufort scale).

Data on the number of birds present during tows or capture events, or how and where in/on the net the capture occurred were not available (Baird & Doonan 2016), although this information is currently being collected (Richard Wells, *pers. comm.*). Note the data on the mesh configuration was that recorded by observers, but we note that these data are uncertain, and may not reflect the actual mesh configuration on each vessel (Richard Wells, *pers. comm.*).

4. METHODS

To estimate risk, a statistical model was developed to estimate the probability of capture for different fishing methods, practices, or mitigation measures. The model here estimated the probability of a capture, and controlled for trends in the data that may have arisen due to spatial and temporal variation in fishing, the type of birds caught, and the type of capture. These factors are not manageable or less likely to be directly relevant to development of mitigation. But ignoring these effects during estimation could introduce bias into the parameter estimates and hence the conclusions. For example, some vessels may catch fewer birds not because of the mitigation strategy in place, but because they are fishing in a particular location or at a particular time where the risk of capture is already low. Ignoring this spatial or temporal effect could exaggerate (and hence bias) the apparent effectiveness of any mitigation measures being used. Similarly, mitigation strategies may preferentially effect different bird groups. Ignoring this effect could result in the estimates of the effectiveness of a strategy being biased by the availability of different bird species at the time of fishing.

4.1. Base model

An initial Base model was developed to represent captures in the squid and middle-depth trawl fisheries distributed over space and across species groups. An explicit representation of time (i.e., the fishing year) was not included since this would be confounded with, and therefore potentially obscure, temporal changes in fishing practices, including the introduction of new mitigation strategies. To control for other temporal effects, such as low resolution changes in the population

size and observer recording practices, only recent data were considered (i.e., post-2007/08 fishing year). All captures were modelled, with the probability of net capture by species group included as estimated parameters. This is an inclusive approach to the analysis, since non-net-captures will still convey information on the distribution of birds across space and their availability for capture. Visual inspection of the empirical plots showed that the conditional probability that a capture was a net capture was consistent over space and time.

Observers record captures per fishing event, with these captures being assigned to one or more discrete categories, namely the species, type of capture and whether the bird was alive or dead (referred to as the "status"). Per fishing event i, we therefore have a conditional multinomial observation process (Equation 1). If the number of captures n_i is treated as a Poisson distributed random variable (Equation 2) then the unconditional multinomial can be represented as a series of Poisson distributions with the rate parameter $\lambda > 0$ representing the expected captures across categories, per tow:

$$\begin{aligned} y_{i1} &\sim P(\pi_1 \cdot \lambda) \\ y_{i2} &\sim P(\pi_2 \cdot \lambda) \\ &\vdots \\ y_{ik} &\sim P(\pi_k \cdot \lambda) \end{aligned} \tag{4}$$

The probability mass function for the above Poisson data y_{ik}, is:

$$\mathbb{P}[y_{ik}] = (\pi_k \cdot \lambda)^{y_{ik}} \cdot \frac{\exp(-\pi_k \cdot \lambda)}{y_{ik}!} \tag{5}$$

Observation categories k were defined according to the non-overlapping species/capture type/status combination (because each recorded capture has a unique assignment to one of these) and the data were summed according to j discrete covariate categories. For the Base model, strata were defined according to the grid g, season r, and target fishery q:

$$z_{jk} = \sum_{i \in rgq} y_{ik}$$

$$E_j = \sum_{i \in rgq} i$$

Since the sum of a Poisson random variable is also Poisson, the probability distribution then becomes:

$$\begin{aligned} z_{j1} &\sim P(\pi_1 \cdot \lambda \cdot E_j) \\ z_{j2} &\sim P(\pi_2 \cdot \lambda \cdot E_j) \\ &\vdots \\ z_{jk} &\sim P(\pi_k \cdot \lambda \cdot E_j) \end{aligned} \tag{6}$$

The probability mass function of these data is:

$$\mathbb{P}\left[z_{jk}\right] = (\pi_k \cdot \lambda \cdot E_j)^{z_{jk}} \cdot \frac{\exp(-\pi_k \cdot \lambda \cdot E_j)}{z_{jk}!} \tag{7}$$

which has the benefit of being much more efficient to compute (since the observations are summed rather than having their likelihoods calculated individually).

As noted by the Fisheries New Zealand Aquatic Environment Working Group (AEWG, 26th November 2020), the model described in Equations 4 and 6 could also be represented using a Negative Binomial probability distribution. The Poisson distribution assumes that the mean and the variance are equal. If the variance is greater than the mean (referred to as "over-dispersion"), then the Negative Binomial may be more appropriate because it includes an extra parameter to allow for the over-dispersion.

A causative mechanism for over-dispersion may be the occurrence of multiple non-independent captures per capture event and Table 2 gives the empirical over-dispersion estimates by capture type, species group and target fishery. Inspection of the table suggests that the over-dispersion was variable and only prominent for MED net captures in the SQU fishery.

Similar to the Poisson distribution, the sum of Negative Binomial random variables is also a Negative Binomial, and we propose that a suitable model could therefore be:

$$\begin{aligned} z_{j1} &\sim NB(\pi_1 \cdot \lambda \cdot E_j, \delta_1) \\ z_{j2} &\sim NB(\pi_2 \cdot \lambda \cdot E_j, \delta_2) \\ &\vdots \\ z_{jk} &\sim NB(\pi_k \cdot \lambda \cdot E_j, \delta_k) \end{aligned} \tag{8}$$

noting that the over-dispersion parameter δ_k is specific to the observation category.

When fitting to the data we used the following probability mass function for the Negative Binomial distribution:

$$\mathbb{P}\left[z_{jk}\right] = \frac{\Gamma(z_{jk}+\delta_k)}{\Gamma(z_{jk}+1)\cdot\Gamma(\delta_k)} \cdot \left(\frac{\delta_k}{\delta_k+\alpha_{jk}}\right)^{\delta_k} \cdot \left(\frac{\alpha_{jk}}{\delta_k+\alpha_{jk}}\right)^{z_{jk}} \tag{9}$$

which is paramaterised using δ_k and the expected value $\alpha_{jk} = \pi_k \cdot \lambda \cdot E_j$.

Table 2: Mean and variance in the capture rate per capture type, species group and target fishery. The over-dispersion is calculated as the variance to mean ratio and is notably high for MED Net captures in the SQU fishery, which also has a large number of multiple capture events.

Capture type	Spp. group	Target	Capture rate		Over dispersion	Number of single captures	Number of multiple captures	Total Captures
			Mean	Variance				
Net	LALB	HHL	0.00	0.00	0.00	0	0	0
	LALB	SQU	<0.005	<0.005	0.40	3	1	5
	MED	HHL	0.02	0.01	0.57	93	20	141
	MED	SQU	0.10	0.72	7.47	817	258	1659
	SALB	HHL	0.01	<0.005	0.04	47	1	49
	SALB	SQU	0.03	0.01	0.18	426	31	494
	SML	HHL	<0.005	<0.005	0.40	3	1	5
	SML	SQU	<0.005	<0.005	0.00	12	0	12
Other	LALB	HHL	0.00	0.00	0.00	0	0	0
	LALB	SQU	<0.005	<0.005	0.00	3	0	3
	MED	HHL	<0.005	<0.005	0.86	4	1	7
	MED	SQU	<0.005	<0.005	0.11	16	1	18
	SALB	HHL	0.01	<0.005	0.17	38	4	46
	SALB	SQU	0.01	0.01	1.25	81	21	144
	SML	HHL	<0.005	<0.005	0.80	5	2	10
	SML	SQU	<0.005	<0.005	0.00	3	0	3

For both the Poisson and Negative Binomial assumptions, we are required to define the partitions for λ, which describe the generative process responsible for captures (e.g., Abraham & Richard

2019, Equation 1). For the Base model this is:

$$\eta(\lambda_j) = \mu + x_q \cdot \beta_q + x_g \cdot \beta_g + x_r \cdot \beta_r \tag{10}$$

for covariate factor levels:

$$\begin{aligned} q &= \{\text{SQU}, \text{HHL}\} \\ g &= \{1, 2, \ldots, 316\} \\ r &= \{\text{Spring}, \text{Summer}, \text{Autumn}, \text{Winter}\} \end{aligned}$$

where η is the link function and x are the covariate data associated with each factor. The notation $x \cdot \beta$ can be interpreted as a series of indicator variables, where x is 0 or 1, depending on the factor level being represented. For example, for the target fishery:

$$x_q \cdot \beta_q \equiv x_{\text{HHL}} \cdot \beta_{\text{HHL}} + x_{\text{SQU}} \cdot \beta_{\text{SQU}}$$

For the middle-depth trawl fishery, $x_{HHL} = 1$ and $x_{SQU} = 0$. Similarly, $x_{HHL} = 0$ and $x_{SQU} = 1$ for the squid fishery. All coefficients were constrained to sum to zero for this and all the models examined.

4.2. Base$^+$ model

The fishing fleets can be grouped into at least three classes based on their size (greater or less than 100 m in length), whether they use bottom or mid-water trawl gear, and whether they have a meal processing plant on board (Richard Wells, *pers. comm.*). The primary groups being:

1. Midwater trawls, ≥ 100 m;
2. Bottom trawls, $43 - 100$ m, with a meal plant; and,
3. Bottom trawls, $43 - 100$ m, without a meal plant.

The trawl type and vessel length are recorded routinely in the commercial effort data, but the presence of a meal plant is only recorded in the observer data, meaning that coverage of the fleets is partial. To characterise these data we therefore defined "Vessel class" as a combination of the gear type and length ("large" vessels being ≥ 100 m and "medium" being $43 - 100$ m). The presence of a meal plant was specified as "Meal", "Not-Meal" or "Unknown". The Base$^+$ model is therefore:

$$\eta(\lambda_j) = \mu + x_q \cdot \beta_q + x_g \cdot \beta_g + x_r \cdot \beta_r + x_v \cdot \beta_v + x_w \cdot \beta_w \tag{11}$$

for additional covariate levels:

$$\begin{aligned} v &= \{\text{Midwater/Large}, \text{Midwater/Medium}, \text{Bottom/Large}, \text{Bottom/Medium}\} \\ w &= \{\text{Meal}, \text{Not Meal}, \text{Unknown}\} \end{aligned}$$

In the case of the β_w covariate:

$$x_w \cdot \beta_w \equiv x_{\text{Meal}} \cdot \beta_{\text{Meal}} + x_{\text{Not Meal}} \cdot \beta_{\text{Not Meal}}$$

When there were missing data (i.e., $w = \text{Unknown}$), both $x_{\text{Meal}} = 0$ and $x_{\text{Not Meal}} = 0$, meaning that $x_w \cdot \beta_w = 0$. With a sum-to-zero constraint on the coefficients $\beta_{\text{Meal}} + \beta_{\text{Not Meal}} = 0$. Therefore β_{Unknown} does not need to be estimated. Instead, the contribution of β_{Unknown} was assumed to be equal to zero, which was the mean of the other covariate values.

Since many of the covariates examined contained missing data, using this "missing indicator" approach we were able to retain data in the analysis even if a particular covariate was missing. The alternative, which would have been to drop missing data, could lead to a loss of statistical power.

4.3. Evaluation of management measures

From Equation 11, we are able to expand the model by including additional behavioural or management-related covariates. Using the generic subscript m, we can write:

$$\eta(\lambda_{j,m}) = \mu + x_q \cdot \beta_q + x_g \cdot \beta_g + x_r \cdot \beta_r + x_v \cdot \beta_v + x_w \cdot \beta_w + x_m \cdot \beta_m \tag{12}$$

Quantification of the risk associated with a particular management-based covariate can then be reduced to estimation of the vector of coefficients β_m.

There are different ways to measure the risk, each of which requires a different link function. For example, using the canonical log-link function: $\eta = \log(\lambda)$ (suitable for both the Poisson and Negative Binomial models), we are able to equate the regression coefficients directly with an expected number of captures. Therefore, we can calculate an "effect size" as the change in capture rate associated with the presence of a particular covariate value. Given that $\lambda_{j,m}$ is the expected total capture rate across observation categories:

$$\text{Capture rate}|j,m = \mathbb{E}\left[\sum_k z_{jkm}/E_j\right] = \lambda_{j,m}$$

the change in capture rate due to a particular management measure is:

$$\begin{aligned}\text{Effect size}|m &= \frac{\lambda_{j,m}|m=1}{\lambda_{j,m}|m=0} \\ &= \frac{\exp(\mu + x_q \cdot \beta_q + \cdots + \beta_1)}{\exp(\mu + x_q \cdot \beta_q + \cdots + \beta_0)} \\ &= \exp(\beta_1 - \beta_0)\end{aligned} \tag{13}$$

which is independent of j.

Alternatively, management can be measured using the probability of there being at least one bird capture across observation categories:

$$\text{Probability of capture}|j,m = \mathbb{P}_{i\in j,m}\left[\left\{\sum_k y_{ik}\right\} > 0\right] = p_{j,m}$$

The ratio of the probability of an event occurring to the probability of the event not occurring is known as the odds:

$$\text{Odds}|j,m = \frac{p_{j,m}}{1-p_{j,m}}$$

Using an appropriate link function η (Table 3 and Sroka & Nagaraja 2018), the risk (expressed as odds) can be related directly to the exponent of the regression coefficients, giving:

$$\begin{aligned}\text{Odds Ratio}|m &= \frac{p_{j,m}|m=1}{p_{j,m}|m=0} \\ &= \exp(\beta_1 - \beta_0)\end{aligned} \tag{14}$$

Table 3: Link functions and model diagnostic calculations for Poisson and Negative Binomial (NB) models. For clarity we use the notation $\alpha = \mu + \cdots$ to represent the regression coefficients.

Prob. mass function	Link function $\eta(\lambda)$	Capture rate $\eta^{-1}(\alpha)$	Prob. capture p
Poisson	$\log(\exp(\lambda)-1)$	$\log(\exp(\alpha)+1)$	$1-\exp(-\lambda)$
NB	$\log\left(\left(1+\frac{\lambda}{\delta}\right)^{\delta}-1\right)$	$\left(\sqrt[\delta]{\exp(\alpha)+1.0}-1.0\right)\cdot\delta$	$1.0-\left(\frac{\delta}{\delta+\lambda}\right)^{\delta}$

These both represent equally valid estimates of the consequences associated with the presence/absence of a particular management measure. For the current work, we adopted the odds ratio (Equation 14) as the starting point for developing our measure of the risk. Since the odds ratio is difficult to interpret intuitively, we have converted it to a measure of the probability of an event taking place (see Appendix C). We calculate the relative risk for factor level m as:

$$R_m = \frac{\exp(\mu+\beta_m)}{1+\exp(\mu+\beta_m)} \tag{15}$$

which we compare to a reference value $R_{REF} = \exp(\mu)/(1+\exp(\mu))$.

4.4. Estimation

Estimation was performed within a Bayesian framework using rstan (Stan Development Team 2020, R Core Team 2020). For each model fit, two parallel chains were run for 2000 iterations with convergence assessed visually. Standard normal priors were assumed for all model coefficients except the intercept term μ for which we assumed an unbounded (improper) uniform distribution. For diagnosing the model fit, we used both the capture rate and the probability of capture (Table 3). Both the capture rate and probability of capture can be disaggregated into different observation categories using the estimated π_k values. This a notable strength of the model, which we use to report model fits by capture type, species group (observation categories) and target fishery (a predictor of the overall capture rate).

4.5. Power analysis

The definition of experimental power is the probability of rejecting a null-hypothesis given that it is false. It is typically calculated as a function of both the effect size and the sampling effort. The larger the effect size being looked for, and the more effort being expended to detect it, the greater the power. Although it can be defined in terms of the regression coefficients i.e., the probability of correctly concluding that a coefficient is significant, in the current setting we define power in terms of the probability of detecting a change in the rate of bird capture. We choose to measure the effect in terms of the capture rate (rather than the probability of capture) because the mean capture rate has a well-defined probability distribution which can be used to estimate the power.

If we have n capture observations $X_1, X_2, \cdots, X_n$ drawn from a Poisson distribution with parameter λ, then the mean number of observations $\bar{X}$ follows a normal distribution with location parameter equal to the rate parameter λ and scale $\sigma = \sqrt{\lambda/n}$, where n is the number of observations. To perform a power test, we calculate from the regression outputs expected capture rates assuming the

null and alternative hypotheses, H_0 and H_1 respectively:

$$\begin{aligned} \lambda|H_0 &= \eta^{-1}(\mu) \\ \lambda|H_1 &= \eta^{-1}(\mu + x_m \cdot \beta_m) \end{aligned} \tag{16}$$

where β_m is the coefficient for factor level m and η^{-1} refers to the inverse link function (Table 3). We are then able to estimate statistical power based on an assumption that $\lambda|H_0$ and $\lambda|H_1$ are the location parameters for two normal distributions.

Performing a one-tailed test, the lower 5% quantile of the null distribution is $q_0 = -1.644854 \cdot \sigma + \lambda_0$, using the notation λ_0 to refer to $\lambda|H_0$. The probability of rejecting the null hypothesis that λ_0 is correct is the integral of the alternate distribution between negative infinity and q_0. The power is therefore:

$$\text{Power to reject } \lambda_0 = \Phi\left(q_0, \lambda_1, \sqrt{\lambda_1/n}\right)$$

where $\Phi(.)$ is the cumulative distribution function for a normal distribution with location λ_1 and standard error $\sqrt{\lambda_1/n}$. The larger the value of the estimated effect size β_m the larger the difference between λ_0 and λ_1 and the great the power. Similarly, the larger the sample size n, the "thinner" the null and alternate distributions and the greater the power.

We generated estimates of statistical power for each estimated coefficient value and for a sampling effort of $n = \{10, 20, \ldots, 10000\}$. This was repeated using the full posterior distribution of each model coefficient, with the final power estimate reported as a mean across posterior samples. We note that this procedure utilises the full posterior or each coefficient estimate and therefore accommodated the statistical uncertainty associated with the model fit. This means that if a posterior distribution of the coefficient estimate overlaps with the reference value then the estimated statistical power may be less than one, even as the proposed sample size increases to infinity. The asymptotic power will therefore depend on the width of the posterior and the precise shape of the posterior will influence the rate at which this asymptote is reached.

5. RESULTS

To inform our analysis we first generated exploratory plots of the mean capture rate per tow (considering all captures) against the available covariate data. Error bars were constructed as 90% quantiles assuming that captures follow a Poisson distribution with rate parameter equal to the mean empirical rate. Plotting the data in this way also provided an opportunity to use discrete categories for the continuous covariates so that they could be more easily modelled.

5.1. Empirical Data

Net configuration: Figure 3 shows the bird capture rates for different net configurations. Preliminary groupings were constructed for the mesh sizes (lengthener and codend), plus the headline height and sweep length. However, there appeared to be limited contrast in the data to suggest that formal modelling was warranted and these covariates were not considered further. For the mesh configurations some patterns were evident, specifically higher catch rates for the Diamond and Square net configurations in both the lengthener and the codend. When modelling these data, warp strikes and other captures were not included.

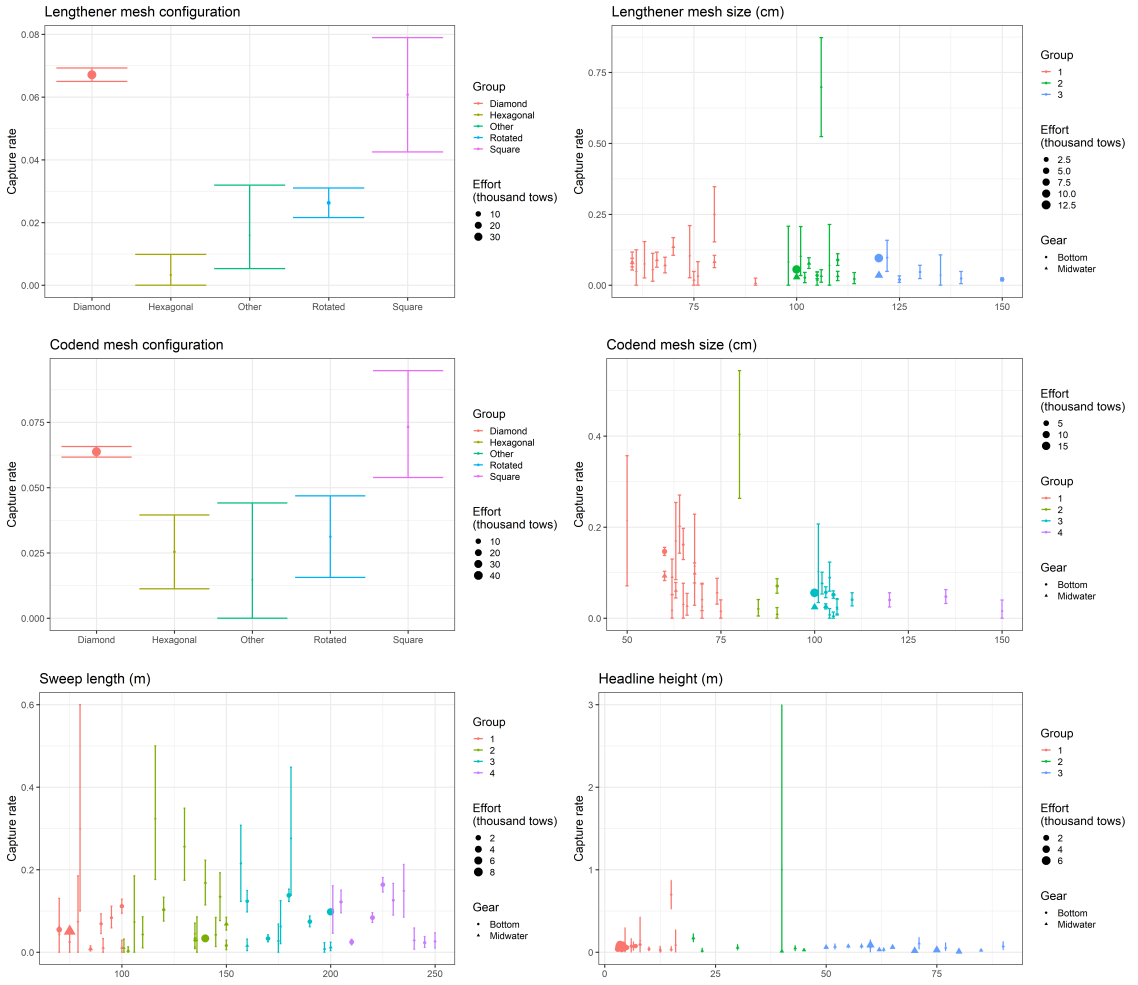

Figure 3: Observed seabird capture rate for the net covariate data (lengthener mesh configuration and size, codend mesh configuration and size, sweep length, and headline height), showing the empirical capture rate against different factor levels.

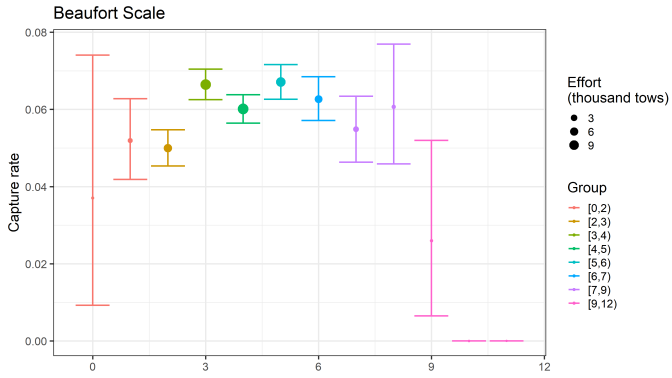

Figure 4: Observed seabird capture rate by Beaufort scale of weather conditions. Beaufort scale value were combined to create groups appropriate for the model fit.

Weather conditions: Empirical plots of the effect of weather conditions, as measured by the Beaufort Scale are shown in Figure 4. It appeared that capture rates were highest at intermediate levels of the Beaufort scale (between 3 and 6), although there was a paucity of data at the extremes.

Time of haul: The capture rate per hour of haul was grouped according to the time of day (dawn/day/dusk/night), calculated using the times of sunrise and sunset for the day of the year and latitude of the haul. Dawn was defined as any time from midnight until an hour after sunrise, dusk as between one hour before and after sunset. Since times of sunrise and sunset change by season, the data were grouped accordingly into season of equal duration, with Summer defined as being from December to February inclusive. The empirical catch rates are shown in Figure 5. Some patterns can be discerned. For example, catch rates appear to be higher during the Autumn, and to a lesser extent, during Summer. It also appears that capture rates at dusk are consistently higher than capture rates at dawn.

Moon phase: The empirical catch rate plotted against the moon phase (Figure 6) showed there was very little discernible difference and was therefore not investigated further.

Surface time: From Figure 7 the capture rate appeared to increase with the time that the net was on the surface during hauling. This would be consistent with intuition, since the longer the surface time the greater the opportunity for birds to feed off the net and become caught.

Fishing effort: The sum of the commercial fishing effort per grid, per year and per day was assigned as a covariate to the capture data. Figure 8 shows the relationship between the empirical capture rate and this local commercial fishing effort. There appears to be an intuitive relationship whereby local effort, as it increased, also lead to an increase in the capture rate, presumably because more birds are attracted. At higher effort levels, the capture rate dropped off, which could potentially be explained as a dilution effect when large numbers of vessels were present.

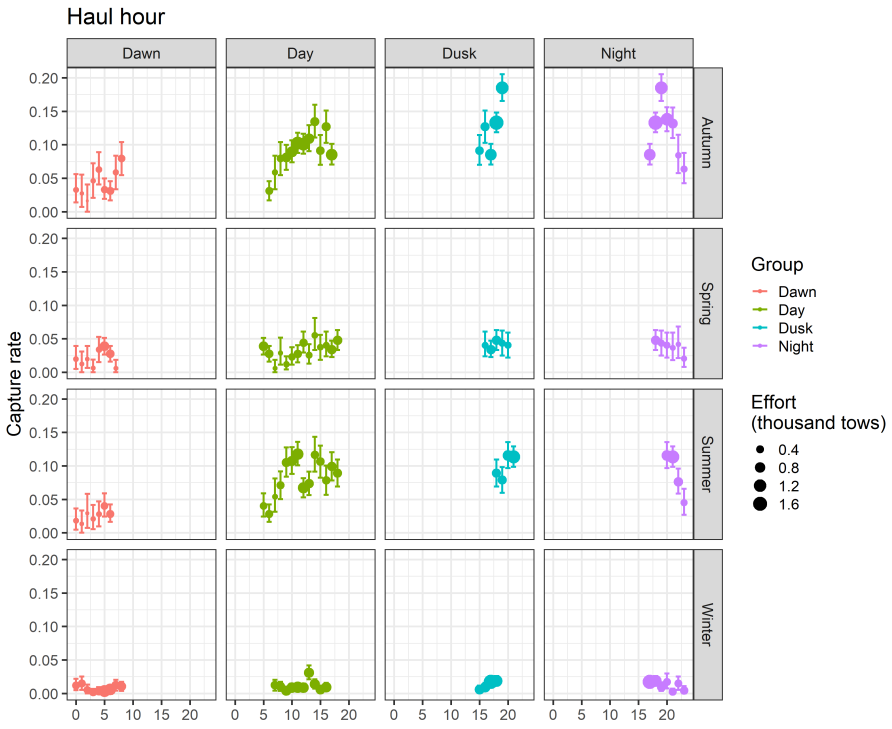

Figure 5: Observed seabird capture rates plotted against the hour of hauling and grouped according to the season (Spring, Summer, Autumn, and Winter) and time of day (dawn, day, dusk, and night). There was some overlap in the groupings since the time of sunrise/sunset depends on the latitude, which was not accounted for in the analysis.

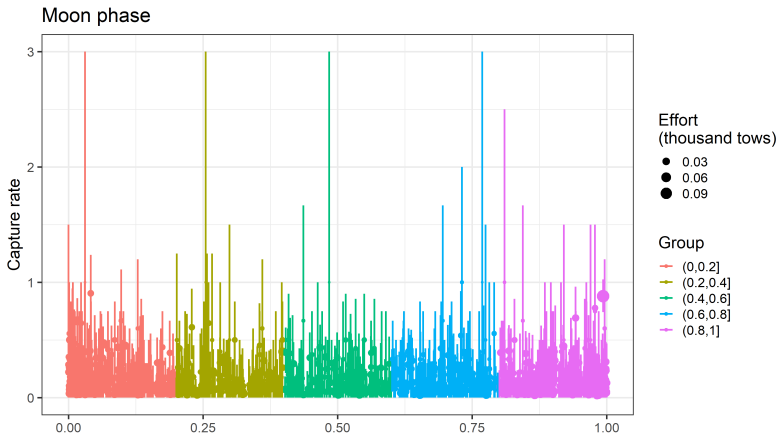

Figure 6: Observed seabird capture rate plotted against the moon phase. The moon phase has been grouped as a preliminary step towards including it as a model covariate.

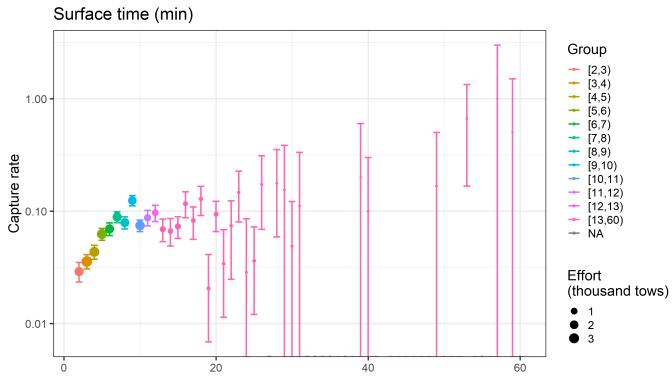

Figure 7: Observed seabird capture rate against time of net on the surface during hauling. Capture rates are shown on a log_10 scale for clarity of presentation.

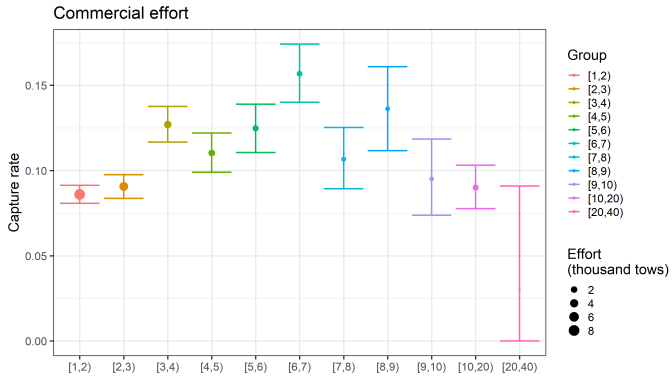

Figure 8: Observed seabird capture rate by commercial effort (number of tows) in the same grid during the same day. Commercial effort has been grouped prior to inclusion as a model covariate.

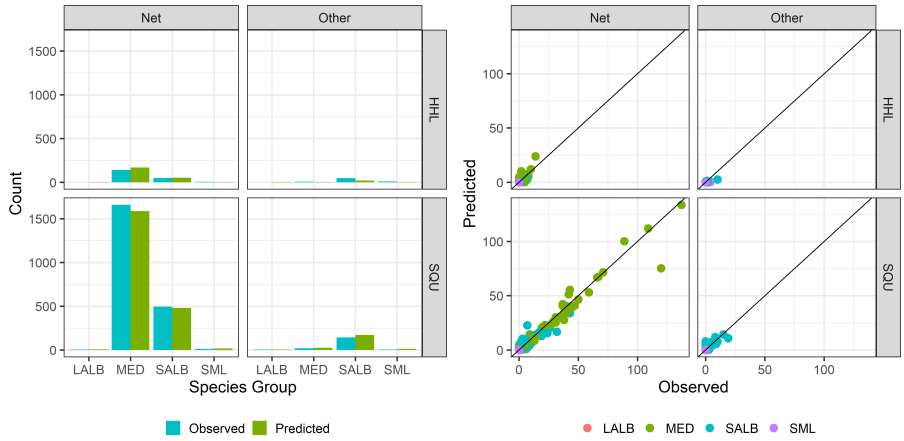

(a) Base Poisson model

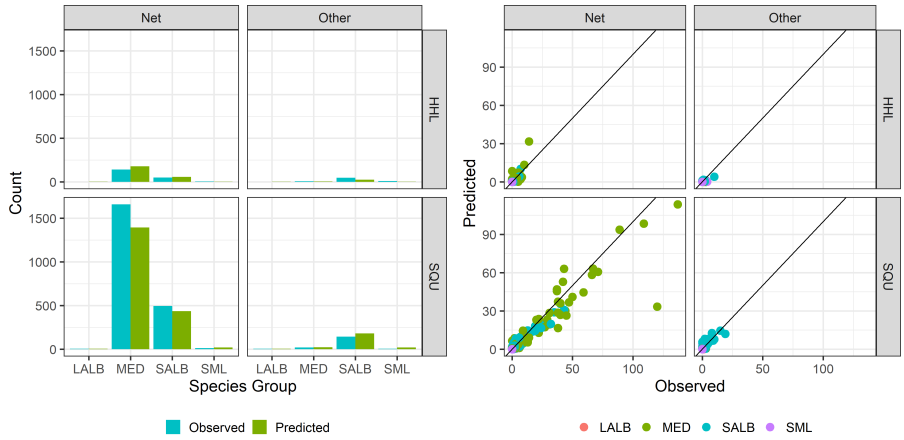

(b) Base NB model

Figure 9: Comparison of the predicted captures from the Base model to the empirical captures per species group, grid and capture type.

5.2. Model fits

Initially, we fitted the Base model using both the Poisson and Negative Binomial assumptions, to determine if it was able to adequately describe the capture data. The overall relationship between observed and predicted captures is shown in Figure 9, with the observed and predicted probabilities of capture shown in Figure 10. Predicted captures over space are shown in Figure 11. The ability of the Base model to predict capture probabilities demonstrated that it was adequate and would provide an approach to evaluate risk at a variety of scales and levels of disaggregation. It may be that future model modifications could be developed that would provide a better fit — for example by allowing a more flexible representation of the observation probabilities π_k, which are currently assumed to be constant across all captures.

Overall, the Poisson model provided a better prediction of the capture rate, whereas the Negative Binomial model provides a better representation of the capture probability. For this reason the Negative Binomial model was retained for further downstream analyses.

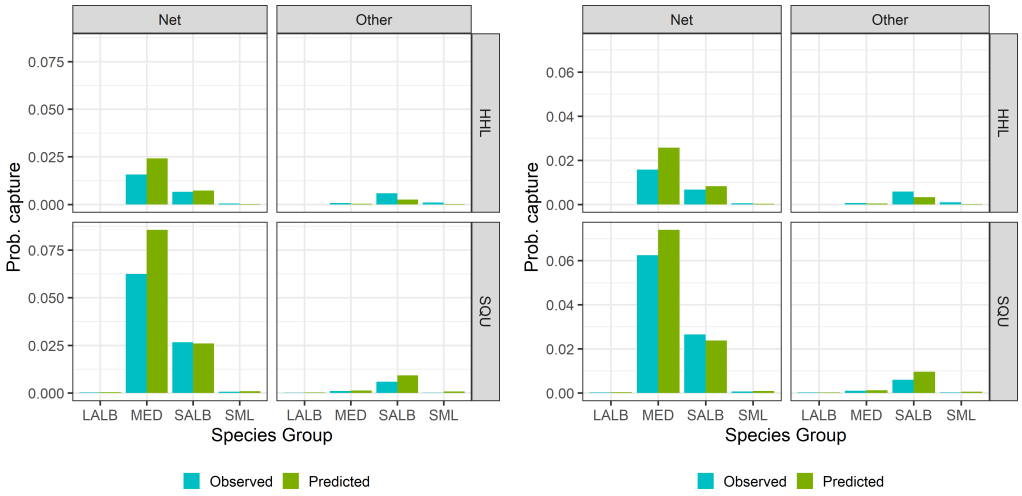

(a) Base Poisson model

(b) Base NB model

Figure 10: Observed and predicted capture probabilities for the Base model by capture type, target, and species group.

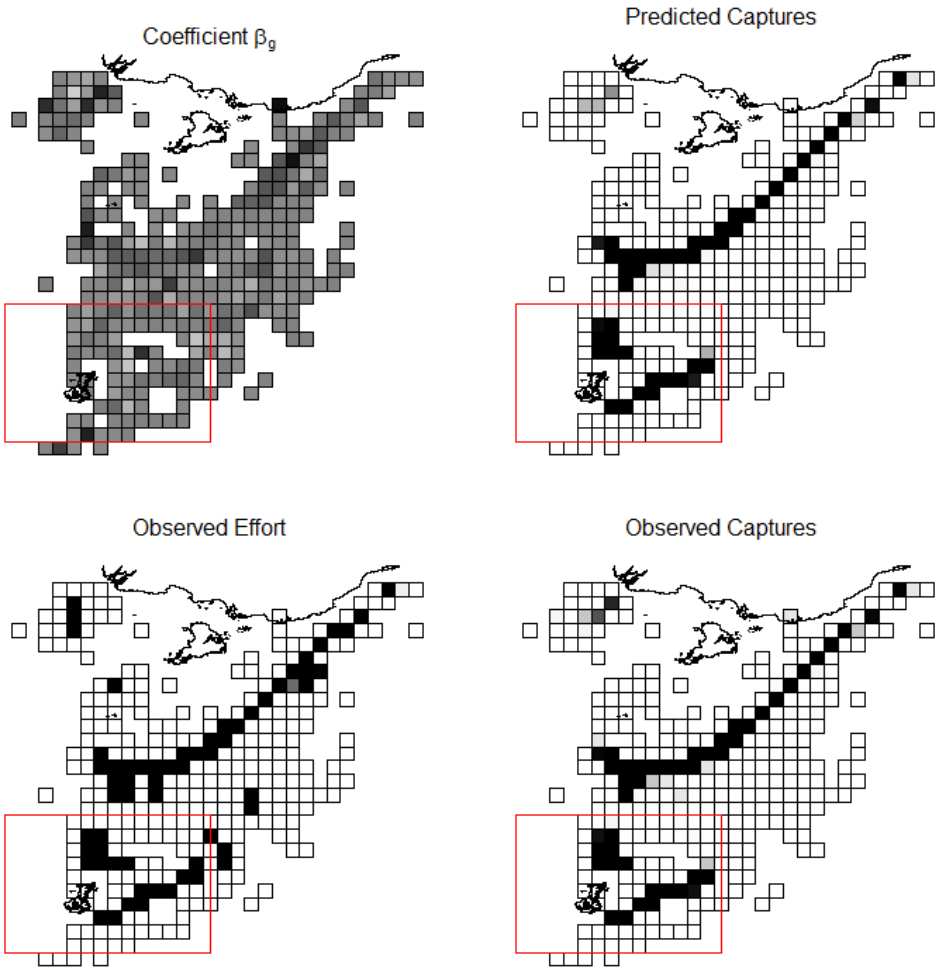

Figure 11: Spatial diagnostics for fit of Base Poisson model to the seabird capture data. All captures and effort are summed across time and target fishery, capture type, and species group. Values were scaled using an inverse-logit transform prior to plotting, and are shown per $0.2^\circ \times 0.2^\circ$ grid. Higher values are shown as darker colours. The red box represents the SQU 6T fishing area.

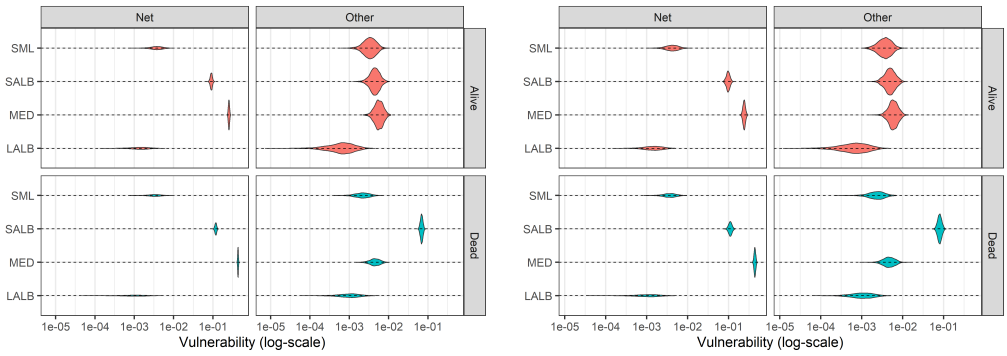

(a) Base Poisson model

(b) Base NB model

Figure 12: Violin plots showing the Base model posterior probability distributions of vulnerability parameters π_k.

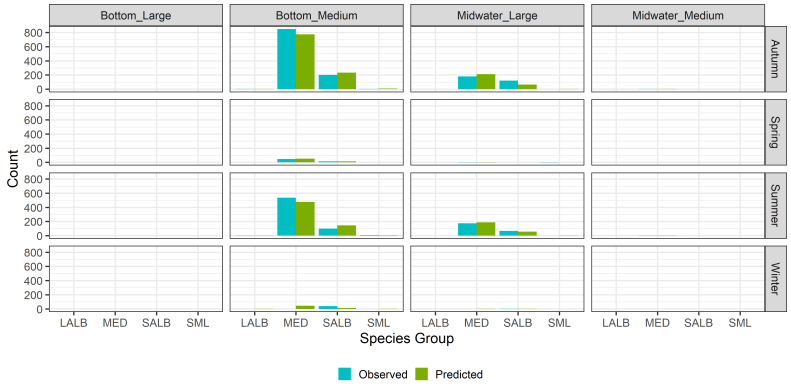

Figure 13: Observed and predicted fits for the Base$^+$ model by fleet and season.

Updates to the prior values for β_q and β_r are shown in the Appendix D (Figure A2, A3). Finally, estimates of the vulnerabilities (π_k) are shown in Figure 12. Consistent with the empirical data, the model predicts that the majority of captures, both alive and dead, were net captures from the SALB and MED species groups.

Having established that the model provided a good fit to the capture data, it was extended by including covariates on the vessel size class and waste management (labelled the Base$^+$ model). Posterior updates are shown in the Appendix D (Figure A5 and A6). Reasonable fits to the captures per vessel class were obtained and shown in Figure 13. Comparisons of the prediction error for the Base and Base$^+$ models demonstrated that the additional covariates did not lead to any reduction in predictive power (not shown).

We then proceeded to evaluate marginal effects of each of the potential management measures listed in the data available. For each estimated covariate we report the risk, R_m (Equation 15), which we compared to the reference value (R_{REF}; Appendix C). For each coefficient we calculated a one-tailed Bayesian *probability of direction* p_d (Makowski et al. 2019), which is an index of "effect existence", with higher values indicating stronger evidence for the presence of an effect:

$$p_d = \mathbb{P}\left[R_m < R_{REF}\right] \tag{17}$$

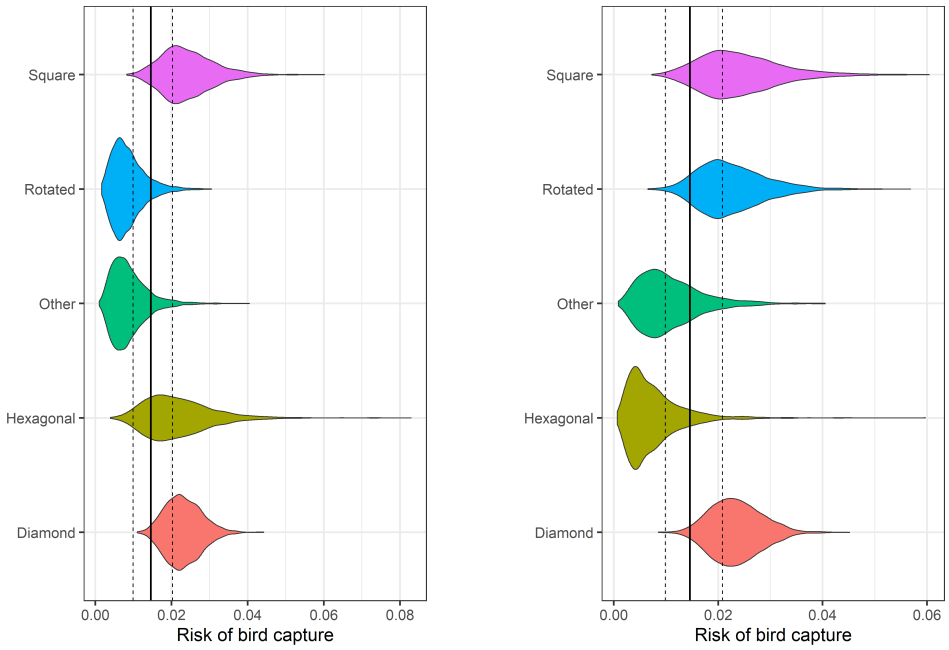

(a) Codend net configuration

(b) Lengthener net configuration

Figure 14: Estimated risk for different codend and lengthener mesh configurations. The "Other" and "Unknown" factor levels are not shown. The R_{REF} is shown as the solid vertical line with 90% credibility intervals.

Net configuration: Estimates of the risk R_m per mesh configuration are given in Table 4 and shown in Figure 14, with the "Other" and "Unknown" factor levels excluded for clarity of presentation. Consistent with the empirical data we estimated the highest risks associated with Diamond and Square mesh configurations. Rotated mesh configurations have the lowest estimated risk in the codend, whereas the Hexagonal mesh has the lowest estimated risk in the lengthener. For the codend, there was strong evidence that the "Rotated" mesh configuration is associated with a reduction in the probability of bird capture ($p_d = 0.93$, Table 4). For the lengthener, evidence was similarly strong for the "Hexagonal" mesh configuration ($p_d = 0.93$).

Weather conditions: Estimates of the risk associated with different weather conditions are shown in Figure 15. Some differences are apparent, with Beaufort scale values > 9 demonstrating a reduced risk of capture, with a p_d value of 1.0 (Table 4).

Time of haul: The risk of capture per time of haul, grouped according to the time of day (dawn/day/dusk/night) and the season is shown in Figure 16. The time of haul is treated as an interaction effect, being dependent on the season (see Figure 5). Risk is therefore also presented by season with a reference risk that is different for each. The p_d values are calculated so as to measure the evidence for an effect for each time of day, within each season and are listed in Table 4. There is evidence to suggest that hauling before dawn represents the lowest associated risk of bird capture.

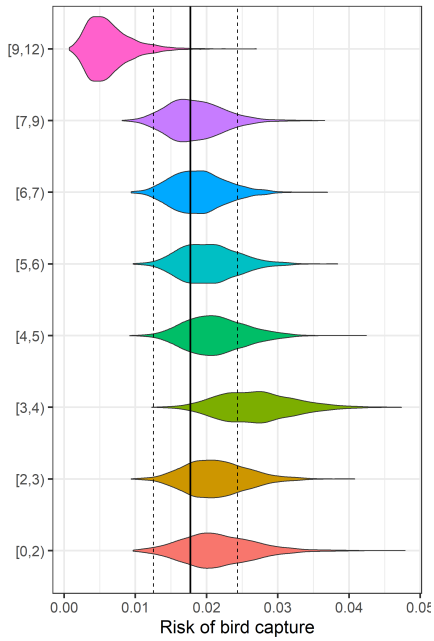

Figure 15: Estimated risk associated with weather conditions during the haul, as measured by the Beaufort scale. The R_{REF} is shown as the solid vertical line with 90% credibility intervals.

Surface time: From the empirical data in Figure 7 we can see that the rate of capture appears to increase with the time that the net is on the surface during hauling, and this is confirmed in our estimate of the risk (Figure 17). There is strong evidence for a reduced risk of capture when surface time is less than 7 minutes (Table 4), with $p_d > 0.9$.

Commercial fishing effort: Figure 18 shows the risk associated with commercial fishing activity in the vicinity of the haul, reducing at higher levels (greater than nine tows), with $p_d > 0.8$.

5.3. Power analysis

Power analyses are useful when designing experiments because they can be used to estimate the probability of detecting an effect, given that the effect is really there. The higher the power, the more likely we are able to detect a significant difference in a future experiment with a given sample size. We note that a power of 80% is traditionally the power used in power analysis studies. This translates as the required sample size for an experiment such that there is an 80% chance that we will significantly detect an effect, given that the effect is really there.

The mean capture rates per effect are listed in Table 4. When estimating statistical power, we estimate the probability that we can accept, in a one-tailed test, the hypothesis that these estimated capture rates were the same as a reference capture rate (the reference rate being calculated with all coefficients set to zero, see Equation 16).

From Figure 19 we can see that power increased with sampling effort for all coefficients that predict a reduction in the rate of bird capture. The larger the reduction, the faster the increase. Because the estimate of power was integrated across the full uncertainty in our estimate of the coefficient (so that some samples from the posterior may still predict an increase in bird capture rate despite an overall reduction) the power may still asymptote at a level less than one. In other words, given

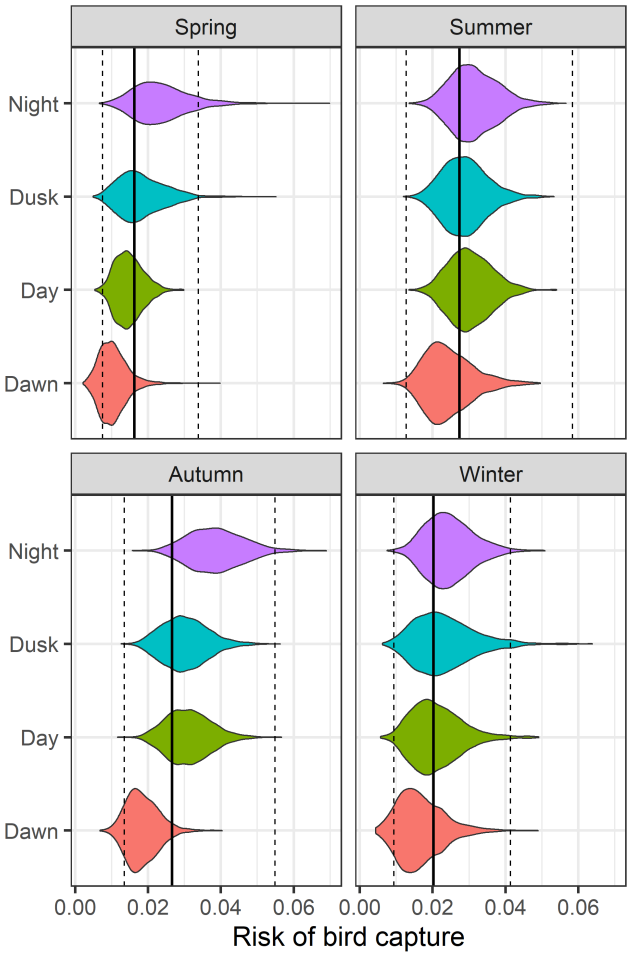

Figure 16: Estimated risk associated with the time of haul. The R_{REF} is shown as the solid vertical line with 90% credibility intervals.

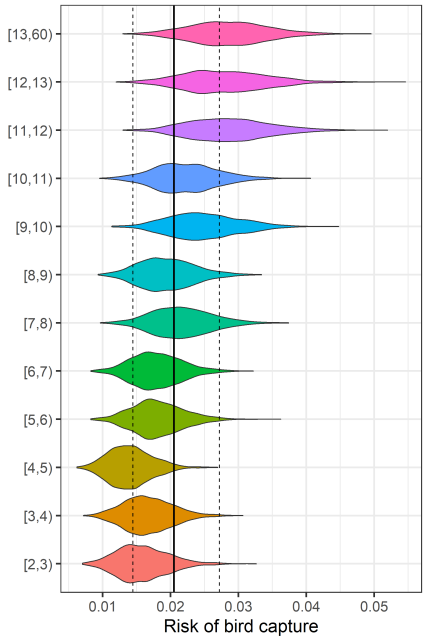

Figure 17: Estimated risk associated with time on the surface during the haul. The R_{REF} is shown as the solid vertical line with 90% credibility intervals.

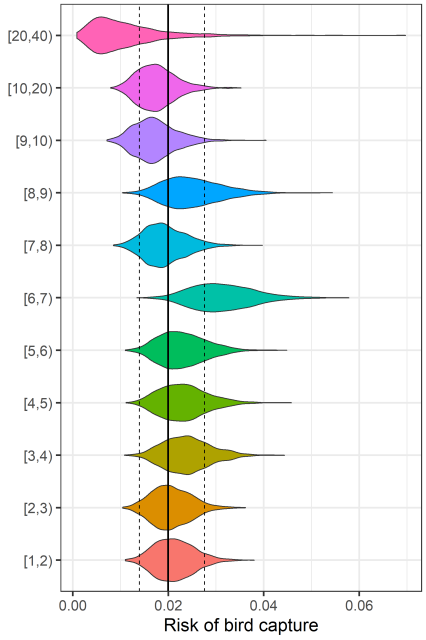

Figure 18: Estimated risk associated with commercial fishing effort in geographical proximity to the haul. The R_{REF} is shown as the solid vertical line with 90% credibility intervals.

uncertainty in the parameter estimates it may never be possible to predict an infallible test. The rate at which the asymptote is approached will depend on the shape of the posterior.

For effect sizes found in the analyses here, the resulting sample sizes to detect an effect are given in Figures 19. Sample sizes for detecting much greater changes would be lower, but given the relatively low rate of captures and the relative risks found in this analyses, detecting such changes in an experiment would require large sample sizes. For example, to detect evidence for a reduction in the capture rate when using Rotated mesh in the codend, we would need in excess of 5,000 observed tows: 2,500 of which would need to be on tows using that particular net configuration. We predict that this would yield a power of 75% (Figure 19a), meaning that there is a 75% probability of rejecting the hypothesis that there is no effect in a one-tailed test.

6. SUMMARY AND CONCLUSIONS

The model developed and presented here is capable of estimating risk as a probability of bird capture, integrating over multiple capture types and species group. This makes it different from other risk assessments conducted in New Zealand (e.g., Richard et al. 2017, 2020), which have concentrated on estimates of the absolute number of bird captures, which is then compared to a reference level of mortality that the population is assumed able to sustain. We have instead calculated a *relative risk*, which does not require information concerning the population sizes of different birds or their spatial distribution. Nevertheless the model is capable of accounting for both spatial and seasonal effects, which are known to correlate with the availability of birds.

The model was inclusive and can make use of multiple types of observational data, and yields an integrated measure of overall risk. With further development, the risk could be disaggregated to, for example, the risk of capturing a particular species group. The multinomial distribution accounted for the fact that different species groups may be caught in different ways, or be more likely caught alive than dead. However it does not account for the fact that these relationships may not be constant over time or space. The relative abundance of different species groups will likely change over time and space, meaning that the probability of a capture being a MED bird, for example, could also change. Future developments of the model will be required to accommodate this uncertainty.

Having constructed a basic model framework that takes into account spatio-temporal effects in the overall probability of bird capture, plus the broad categories of fishing vessel, and showing that it was able to fit the count data well, we then estimated the risk for a variety of covariates. These were selected based on the availability of data, consultation with Fisheries New Zealand and empirical plots of the capture rates. The risk of bird capture per tow is typically in the region of $1-3\%$. The capture rate is similar, reflecting the fact that the majority of bird captures events were single capture events.

In general, results show that there was evidence for an effect of fishing practices on risk in multiple instances, particularly concerning the time that the net is on the surface, but that the overall effect size was small. In other words, even though there may be statistical evidence for a covariate being correlated with a reduction in bird captures, the magnitude of the reduction was small and only of the order of $1-2\%$. The key effects identified were the time that a net remained on the surface, the magnitude of other commercial fishing effort in the local vicinity at the time of the haul (which could potentially be explained as a dilution effect when large numbers of vessels were present), the type of mesh for the codend (with Rotated mesh yielding the lowest probability of capture) and

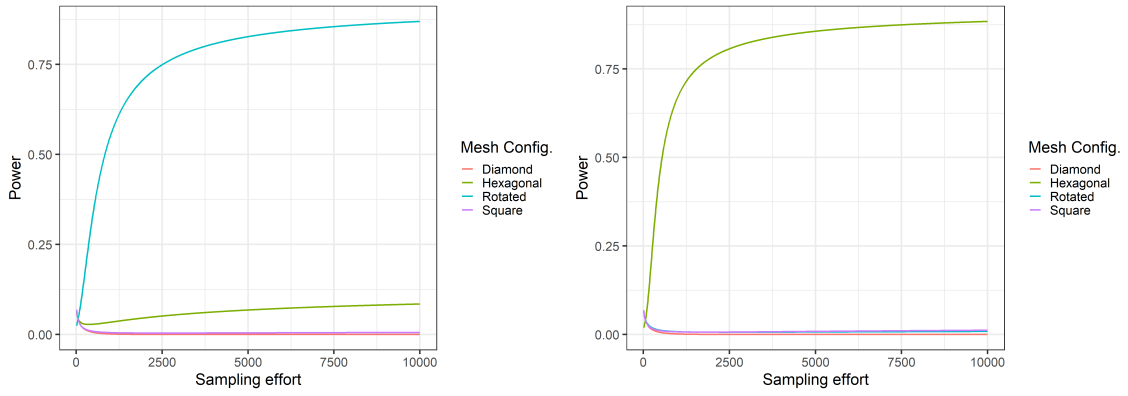

(a) Codend mesh configuration.

(b) Lengthener mesh configuration

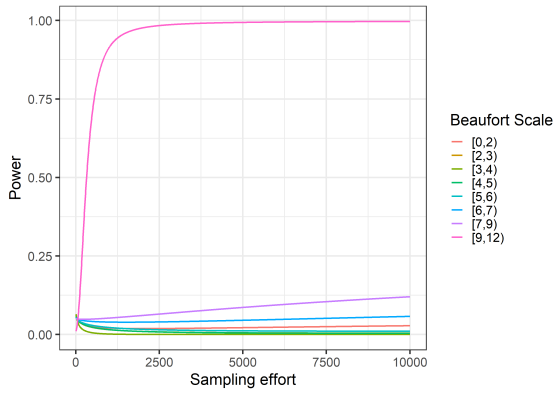

(c) Beaufort scale

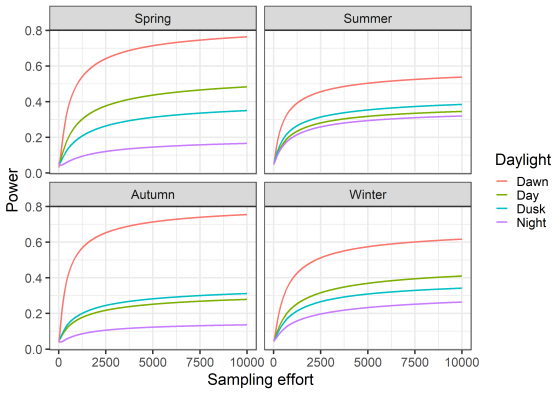

(d) Daylight configuration

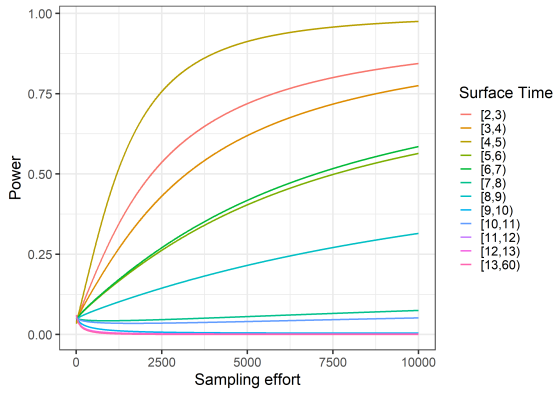

(e) Surface time

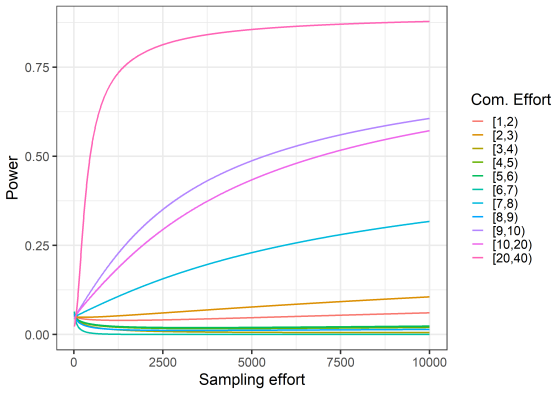

(f) Commercial fishing effort

Figure 19: Estimates of power relative to the sampling effort. Actual sampling effort would need to be double that shown, since samples would be required both for the factor level being tested and other levels (sampled at random), to create a two-sample test of the probability that captures have been reduced.

the type of mesh in the lengthener (with Hexagonal mesh presenting the lowest risk). However, we note that although we have attempted to use models that account for potential confounding between these and other covariates, such as the type of vessel and the time and place of fishing, some unaccounted for interactions may still exist. Further, we note that the data on the type of mesh for the codend may be uncertain and reflect recording practice by observers rather than a significant difference in the mesh construction (Richard Well, *pers. comm.*).

There are additional considerations of relevance to the practical application of the results of this analysis. Minimising the amount of time that the net remains on the surface during hauling is already included within the recommended practice guidelines, and our analyses are consistent with the use of such guidelines and confirms the continued utility of maintaining that practice. Use of alternate mesh configurations also has practical implications concerning integrity of the net, which may need to be considered. However, we recommend that in the first instance, the data recording practice for the mesh construction be reviewed and standardised to assess if this is a real effect or not. The results presented here may nevertheless prove useful in informing fishing practice guidelines that have the potential to further reduce bird bycatch.

6.1. Considerations in the development of designed experiments for trialing alternative mitigation methods

Power analysis allows an experiment to be designed that has a high probability of detecting a treatment effect of a pre-defined magnitude (the "effect size"). In the power analyses described above we have performed a formal evaluation of the probability of detecting a significant effect, given an estimated effect size and for differing experimental sample sizes. This assumes that the effect size is as estimated by the model and that the principles of experimental design are followed during future sample collection. These principles include a requirement that future observations measure the effect of interest (in this case, seabird captures), randomised sampling, a formal hypothesis (i.e., that the new mitigation method will reduce seabird interactions by some predetermined proportion), and a defined statistical method that is used for evaluating the result (in this case a two-sample, one-tailed z-test). Since neither the effect size being tested, nor the statistical method used for the testing, account for the autocorrelation and potential non-independence of confounding factors, they are only indicative of the true sample size that would be required for a designed experiment.

When evaluating a new mitigation method for reducing seabird captures, we are constrained by the actual observed rate of captures (in the case of the New Zealand squid fishery for example, capture rates are very low), and by the practical constraints of trialling these on the fishing vessel fleet. Power analyses assume an ideal randomised design, which may be difficult to achieve in practice, and when the effect size being tested and observation rate of captures are both low, a large sample size can be required.

The power analyses here suggest that for an effect size equivalent to a 2% reduction in seabird capture rate, sample sizes of at least 5000 observed tows would be required to have a 75% chance of correctly concluding that a significant difference exists. With the current number of observed tows at about 1500 per year, this would imply that an optimal experiment would take at least 4 years to obtain adequate data to evaluate a new mitigation method, assuming that all observed vessels were included in the experiment.

While there are techniques to further optimise the design (e.g., Latin square experimental designs), the factors that effect seabird captures are typically highly dependent on the individual vessel and

the individual vessel practise on any given tow. It may therefore be difficult to adequately design an experiment that correctly randomises the mitigation method and controls for multiple effects, especially on a tow-by-tow basis. We note that in the power analysis presented here, we assume that the mitigation method is tied to the vessel effort and that individual tows could not easily be randomised to two or more mitigation methods (for example, if a method were to evaluate an alternative trawl cod-end mesh design, it cannot be varied randomly on a tow-by-tow basis for an individual vessel, but rather would likely be randomly allocated on a vessel trip basis). Alternatively, if a mitigation method could be deployed on a single tow on a random allocation basis, then this would result in a sample size that would likely be lower to determine detect an effect size where one exists. However, given the low rate of seabird captures, the influence of effects from location, season, time of day, and vessel gear configuration, the number of observations would still likely be very high.

New mitigation methods may conceivably increase as well as decrease bird capture rates, and one aspect that is commonly found in medical studies, where experimental designs are well constructed and highly controlled, are "stopping rules." These are often implemented to avoid the potential for severe adverse effects. These can however, bias the outcome. For example, if in a study the data are evaluated prior to completing the sample collection stipulated by the design, an effect is often found by chance alone – even if, should the study complete, the overall effect is insignificant (Deichmann et al. 2016). In the case of seabird captures, we would recommend that if a trial be undertaken, periodic evaluation takes place to determine if the new mitigation method has a severe adverse effect, but without evidence that it does, the trial be continued until its design is complete.

The exact method of design would depend on the mitigation method. In particular, if the method could be applied to random tows per vessel during the course of its operations, or if it can only be applied to each vessel trip or each vessel in turn. Randomised designs on a tow-by-tow basis would be statistically more efficient (i.e. require a smaller sample size) but would require rigorous protocols around its implementation. Randomisation across vessel trips would be more likely, as most mitigation methods would likely apply to the specific gear configuration. Randomising across vessels would be the least efficient approach. It would be unlikely to result in a conclusive effect as there would remain uncertainty over the practise of vessels with and without the proposed mitigation method as the two factors are likely to be highly correlated.

In general, the approach to experimental design would (a) include as many observed tows (and hence observed vessels) as possible with a target of about 2500 tows per method (i.e., for a new mitigation method, then the sample size would be about 5000 tows in order to test the new method against the capture rate for tows that don't use it), (b) would require a rigorous experimental protocol and data recording practise on each vessel that would be mitigation method specific, and (c) would take place over a number of years (i.e., at least 3–4 years), with annual evaluation of severe adverse effects that would inform stopping criteria to avoid continuing testing a mitigation method that could result in a higher rate of seabird captures.

6.2. Considerations for current data collection practices

We note that current data collection practices have allowed us to perform a comprehensive statistical analysis of seabird capture rates. Further work, particularly if new mitigation methods are to be trialled, will require this data collection to be continued and improved upon. Although we have identified instances during this study were some data may have been incorrectly recorded (e.g. net surface times of 2 to 3 minutes; hexagonal mesh in the codend), we note that that the current high standards of data collection will facilitate future experimental work. In addition to the

construction of experiments for the formal evaluation of hypotheses, informal, periodic review and exploratory analyses of these data could prove fruitful. This would allow the data to be continuously interrogated, and emergent patterns further explored.

7. ACKNOWLEDGEMENTS

We thank Fisheries New Zealand in the Ministry for Primary Industries for the help and assistance in interpreting the data used in this report. The data on captures were made available from Fisheries New Zealand and Dragonfly Data Science. We thank Richard Wells (Resourcewise), Daniel Kerrigan (MPI), and the members of the Aquatic Environment Working Group for their helpful input and advice in developing this report. This project was funded by Fisheries New Zealand under project code PSB2018-10.

Table 4: Risk of bird capture for different factor levels.

Factor	Level	Capture rate	Relative Risk	p_d
Codend	Diamond	0.023 (0.016-0.032)	0.023 (0.016-0.031)	<0.001
Mesh config.	Hexagonal	0.021 (0.010-0.039)	0.020 (0.010-0.038)	0.152
	Rotated	0.008 (0.003-0.018)	0.008 (0.003-0.017)	0.932
	Square	0.024 (0.014-0.039)	0.023 (0.014-0.037)	0.015
Lengthener	Diamond	0.024 (0.016-0.033)	0.023 (0.016-0.032)	<0.001
Mesh config.	Hexagonal	0.006 (0.002-0.018)	0.006 (0.002-0.017)	0.925
	Rotated	0.022 (0.014-0.036)	0.022 (0.014-0.034)	0.026
	Square	0.024 (0.014-0.040)	0.023 (0.013-0.038)	0.034
Beaufort	[0,2)	0.022 (0.014-0.032)	0.021 (0.014-0.031)	0.100
scale	[2,3)	0.022 (0.015-0.030)	0.021 (0.015-0.029)	0.019
	[3,4)	0.027 (0.019-0.038)	0.027 (0.019-0.036)	<0.001
	[4,5)	0.021 (0.015-0.030)	0.021 (0.015-0.029)	0.011
	[5,6)	0.021 (0.015-0.028)	0.020 (0.014-0.027)	0.052
	[6,7)	0.019 (0.013-0.027)	0.019 (0.013-0.026)	0.267
	[7,9)	0.019 (0.013-0.026)	0.018 (0.012-0.025)	0.403
	[9,12)	0.006 (0.002-0.013)	0.006 (0.002-0.012)	1.000
Daylight	Autumn/Dawn	0.018 (0.012-0.027)	0.018 (0.012-0.026)	0.847
	Autumn/Day	0.032 (0.022-0.044)	0.031 (0.022-0.042)	0.360
	Autumn/Dusk	0.031 (0.021-0.044)	0.030 (0.021-0.041)	0.392
	Autumn/Night	0.040 (0.028-0.055)	0.038 (0.027-0.052)	0.178
	Spring/Dawn	0.010 (0.005-0.018)	0.010 (0.005-0.017)	0.859
	Spring/Day	0.015 (0.009-0.022)	0.014 (0.009-0.022)	0.598
	Spring/Dusk	0.018 (0.009-0.031)	0.017 (0.009-0.03)	0.448
	Spring/Night	0.023 (0.013-0.039)	0.023 (0.013-0.038)	0.236
	Summer/Dawn	0.024 (0.016-0.039)	0.023 (0.015-0.037)	0.626
	Summer/Day	0.031 (0.022-0.042)	0.030 (0.021-0.040)	0.422
	Summer/Dusk	0.030 (0.020-0.042)	0.029 (0.02-0.040)	0.464
	Summer/Night	0.032 (0.022-0.045)	0.031 (0.022-0.043)	0.392
	Winter/Dawn	0.016 (0.008-0.030)	0.016 (0.008-0.029)	0.714
	Winter/Day	0.021 (0.012-0.035)	0.020 (0.011-0.034)	0.503
	Winter/Dusk	0.023 (0.012-0.041)	0.022 (0.012-0.039)	0.430
	Winter/Night	0.025 (0.015-0.038)	0.024 (0.015-0.036)	0.347
Surface	[2,3)	0.016 (0.01-0.023)	0.016 (0.010-0.023)	0.984
time (min)	[3,4)	0.017 (0.011-0.024)	0.016 (0.011-0.023)	0.985
	[4,5)	0.014 (0.009-0.020)	0.014 (0.009-0.02)	1.000
	[5,6)	0.018 (0.012-0.026)	0.018 (0.012-0.025)	0.934
	[6,7)	0.018 (0.012-0.025)	0.018 (0.012-0.025)	0.949
	[7,8)	0.022 (0.015-0.030)	0.021 (0.015-0.029)	0.306
	[8,9)	0.020 (0.013-0.028)	0.019 (0.013-0.027)	0.781
	[9,10)	0.025 (0.017-0.035)	0.024 (0.017-0.034)	0.018
	[10,11)	0.023 (0.015-0.031)	0.022 (0.015-0.030)	0.215
	[11,12)	0.029 (0.020-0.041)	0.028 (0.020-0.039)	0.001
	[12,13)	0.029 (0.019-0.040)	0.028 (0.019-0.038)	0.007
	[13,60)	0.029 (0.020-0.040)	0.028 (0.019-0.038)	<0.001
Commercial	[1,2)	0.022 (0.015-0.030)	0.021 (0.015-0.028)	0.268
effort (tows)	[2,3)	0.021 (0.015-0.029)	0.020 (0.014-0.028)	0.402
	[3,4)	0.024 (0.017-0.034)	0.024 (0.017-0.033)	0.025
	[4,5)	0.023 (0.016-0.033)	0.023 (0.016-0.032)	0.080
	[5,6)	0.023 (0.016-0.033)	0.023 (0.016-0.032)	0.102
	[6,7)	0.032 (0.022-0.045)	0.031 (0.022-0.043)	<0.001
	[7,8)	0.019 (0.013-0.028)	0.019 (0.013-0.027)	0.652
	[8,9)	0.025 (0.017-0.038)	0.024 (0.016-0.036)	0.052
	[9,10)	0.017 (0.011-0.026)	0.017 (0.011-0.025)	0.854
	[10,20)	0.018 (0.012-0.026)	0.017 (0.012-0.025)	0.874
	[20,40)	0.009 (0.003-0.027)	0.009 (0.003-0.026)	0.917

References

Abraham, E.; Richard, Y. (2019). Estimated capture of seabirds in New Zealand trawl and longline fisheries, 2002–03 to 2015–16. *New Zealand Aquatic Environment and Biodiversity Report No. 211* 99 p.

Abraham, E.; Richard, Y.; Berkenbusch, K.; Thompson, F. (2016). Summary of the capture of seabirds, marine mammals, and turtles in New Zealand commercial fisheries, 2002–03 to 2012–13. *New Zealand Aquatic Environment and Biodiversity Report No. 169* 206 p.

Allard, D.; Comunian, A.; Renard, P. (2012). Probability aggregation methods in geoscience. *Mathematical Geosciences 44*: 545–581.

Baird, S. (2008). Net captures of seabirds during trawl fishing operations in New Zealand waters. (Unpublished NIWA Client Report WLG2008-22 prepared for Clement & Associates Ltd.) 35 p.

Baird, S.; Doonan, I. (2016). Characterisation of seabird captures in trawl nets in New Zealand fisheries, 2008–15. (Unpublished Final Research Report prepared for MPI project DAE2015-01 and held by Fisheries New Zealand, Wellington.) 110 p.

Deichmann, R.; Krousel-Wood, M.; Breault, J. (2016). Considerations for stopping a clinical trial early. *Ochsner Journal 16*: 197–198.

Fisheries New Zealand (2020). Spatially Explicit Fisheries Risk Assessment (SEFRA) - Technical Summary. *Aquatic Environmenta and Biodiversity Annual Review Chapter 3*

Hobday, A.; Smith, A.; Stobutzki, I.; Bulman, C.; Daley, R.; Dambacher, J.; Deng, R.; Dowdney, J.; Fuller, M.; Furlani, D.; Griffiths, S.; Johnson, D.; Kenyon, R.; Knuckey, I.; Ling, S.; Pitcher, R.; Sainsbury, K.; Sporcic, M.; Smith, T.; Turnbull, C.; Walker, T.; Wayte, S.; Webb, H.; Williams, A.; Wise, B.; Zhou, S. (2011). Ecological risk assessment for the effects of fishing. *Fisheries Research 108* (*2*): 372 – 384.

Makowski, D.; Ben-Shachar, M.S.; Lüdecke, D. (2019). bayestestR: Describing Effects and their Uncertainty, Existence and Significance within the Bayesian Framework. *Journal of Open Source Software 4* (*40*): 1541.

R Core Team (2020). R: A Language and Environment for Statistical Computing. R Foundation for Statistical Computing, Vienna, Austria. Version 4.0.2

Richard, Y.; Abraham, E. (2015). Assessment of the risk of commercial fisheries to New Zealand seabirds, 2006-07 to 2012-13. *New Zealand Aquatic Environment and Biodiversity Report No. 162* 85 p.

Richard, Y.; Abraham, E.; Berkenbush, K. (2017). Assessment of the risk of commercial fisheries to New Zealand seabirds, 2006–07 to 2014–15. *New Zealand Aquatic Environment and Biodiversity Report No. 191* 104 p.

Richard, Y.; Abraham, E.; Berkenbush, K. (2020). Assessment of the risk of commercial fisheries to New Zealand seabirds, 2006–07 to 2016–17. *New Zealand Aquatic Environment and Biodiversity Report No. 237* 57 p.

Satopaa, V.A.; Baron, J.; Foster, D.P.; Mellers, B.A.; Tetlock, P.E.; Ungar, L.H. (2014). Combining multiple probability predictions using a simple logit model. *International Journal of Forecasting 30* (*2*): 344 – 356.

Sroka, C.; Nagaraja, H. (2018). Odds ratios from logistic, geometric, Poisson, and negative binomial regression models. *BMC Medical Research Methodology 18* (*112*): 11 p.

Stan Development Team (2020). RStan: the R interface to Stan. Version 2.21.2

APPENDICES

A. DATA TABLES

Table A1: Captures by mortality group

	LALB	SML	SALB	MED	Total
2006/2007	32	14	205	160	413
2007/2008	6	8	90	181	286
2008/2009	5	18	178	295	525
2009/2010	14	20	199	210	450
2010/2011	4	11	109	271	395
2011/2012	15	8	178	108	309
2012/2013	5	15	263	443	726
2013/2014	4	12	202	401	620
2014/2015	3	11	193	475	683
2015/2016	15	13	293	345	680
2016/2017	7	4	155	331	498
Total	110	134	2 065	3 220	5 585

Table A2: Captures by fishing method

	Other	Purse Seine	Set Net	Line	Trawl	Total
2006/2007	0	5	4	212	192	413
2007/2008	0	2	6	63	215	286
2008/2009	0	0	12	86	427	525
2009/2010	0	0	8	192	250	450
2010/2011	0	0	0	64	331	395
2011/2012	0	0	0	69	240	309
2012/2013	0	0	4	33	689	726
2013/2014	2	0	2	131	485	620
2014/2015	0	1	2	65	615	683
2015/2016	1	0	15	228	436	680
2016/2017	0	0	3	100	395	498
Total	3	8	56	1 243	4 275	5 585

Table A3: Captures by capture method

	Other	Paravane	Mitigation device	Tangled	Line	Warp or door	Hook	Net	Total
2006/2007	0	0	1	1	154	18	37	155	366
2007/2008	3	2	5	4	0	22	59	180	275
2008/2009	0	0	8	10	0	55	73	372	518
2009/2010	1	9	2	16	0	42	174	190	434
2010/2011	1	0	1	5	0	16	58	300	381
2011/2012	2	1	3	5	0	63	60	171	305
2012/2013	0	2	4	0	0	66	33	608	713
2013/2014	1	1	1	1	0	65	130	413	612
2014/2015	2	1	7	3	0	21	62	581	677
2015/2016	2	3	0	6	0	43	219	396	669
2016/2017	1	1	4	12	0	23	86	366	493
Total	13	20	36	63	154	434	991	3 732	5 443

Table A4: Captures by target

	OEO	ORH	PEL	SCI	HHL	SQU	Total
2006/2007	0	1	4	21	83	116	413
2007/2008	3	4	4	10	60	150	286
2008/2009	1	5	6	19	57	245	525
2009/2010	6	13	16	4	74	90	448
2010/2011	1	0	18	98	73	130	395
2011/2012	2	0	8	9	77	102	309
2012/2013	0	1	43	6	111	431	726
2013/2014	2	0	22	6	203	206	618
2014/2015	0	0	16	7	101	384	683
2015/2016	1	3	12	3	154	282	680
2016/2017	0	2	9	11	105	244	498
Total	16	29	158	194	1 098	2 380	5 581

Table A5: Captures by area

	WCSI	CHAT	ECSI	AUCK	STEW	Total
2006/2007	15	46	25	48	91	413
2007/2008	13	15	31	55	111	286
2008/2009	14	25	96	140	158	525
2009/2010	38	25	67	22	116	450
2010/2011	4	25	25	128	124	395
2011/2012	36	21	22	46	98	309
2012/2013	43	28	55	156	399	726
2013/2014	44	75	84	45	256	620
2014/2015	30	49	25	102	409	683
2015/2016	89	113	39	131	199	680
2016/2017	60	40	34	80	224	498
Total	386	462	503	953	2 185	5 585

B. SPECIES CODES

Species code	Captures	Common name	Scientific name	Group code
XWC	1 654	White-chinned petrel	Procellaria aequinoctialis	MED
XSH	1 097	Sooty shearwater	Ardenna grisea	MED
XWM	921	White-capped albatross	Thalassarche steadi	SALB
XBM	642	Buller's albatross	Thalassarche bulleri bulleri	SALB
XSA	380	Salvin's albatross	Thalassarche salvini	SALB
XFS	141	Flesh-footed shearwater	Ardenna carneipes	MED
XBP	133	Black (Parkinson's) petrel	Procellaria parkinsoni	MED
XGP	94	Grey petrel	Procellaria cinerea	MED
XWP	55	Westland petrel	Procellaria westlandica	MED
XCM	39	Campbell albatross	Thalassarche impavida	SALB
XCC	38	Cape petrel	Daption capense	SML
XAU	34	Gibson's albatross	Diomedea antipodensis gibsoni	LALB
XAN	30	Antipodean albatross	Diomedea antipodensis antipodensis	LALB
XPP	25	Spotted shag	Phalacrocorax punctatus	DIVE
XAL	23	Albatrosses (Unidentified)	Diomedeidae (Family)	SALB
XRA	22	Southern royal albatross	Diomedea epomophora	LALB
XCI	22	Chatham Island albatross	Thalassarche eremita	SALB
XDP	19	Common diving petrel	Pelecanoides urinatrix	SML
XYP	12	Yellow-eyed penguin	Megadyptes antipodes	DIVE
XNP	12	Northern giant petrel	Macronectes halli	SALB
XGF	12	Grey-faced petrel	Pterodroma macroptera	MED
XFP	12	Fairy prion	Pachyptila turtur	SML
XCP	10	Cape petrels	Daption spp.	SML
XBS	10	Buller's shearwater	Ardenna bulleri	MED
XWF	9	White-faced storm petrel	Pelagodroma marina maoriana	SML
XTP	8	Giant petrels (Unidentified)	Macronectes spp.	SALB
XPR	8	Antarctic prion	Pachyptila desolata	SML
XLB	8	Little blue penguin	Eudyptula minor	DIVE
XBG	8	Black-backed gull	Larus dominicanus	MED
XAG	7	Antipodean and Gibson's albatross	Diomedea antipodensis	LALB
XGB	6	Grey-backed storm petrel	Garrodia nereis	SML
XFU	6	Fulmar prion	Pachyptila crassirostris	SML
XCA	6	Snares Cape petrel	Daption capense australe	SML
XAS	6	Wandering (Snowy) albatross	Diomedea exulans	LALB
XXP	5	Petrels, Prions and Shearwaters	Hydrobatidae, Procellariidae & Pelecanoididae (Families)	SML
XWA	5	Wandering albatross (Unidentified)	Diomedea exulans & D. antipodensis sspp.	LALB

XTS	5	Short-tailed shearwater	Ardenna tenuirostris	MED
XSM	5	Southern black-browed albatross	Thalassarche melanophris	SALB
XPE	5	Petrel (Unidentified)	Procellariidae (Family)	MED
XFL	5	Fluttering shearwater	Puffinus gavia	SML
XSW	4	Shearwaters	Puffinus & Ardenna spp.	MED
XMA	4	Smaller albatrosses	Thalassarche spp.	SALB
XSS	3	Seabird - Small		SML
XSI	3	Stewart Island shag	Phalacrocorax chalconotus	DIVE
XRU	3	Royal albatrosses	Diomedea sanfordi & D. epomophora	LALB
XPN	3	Prions (Unidentified)	Pachyptila spp.	SML
XKM	3	Black-browed albatross (Unidentified)	Thalassarche melanophris & T. impavida	SALB
XFC	3	Fiordland crested penguin	Eudyptes pachyrhynchus	DIVE
XSL	2	Seabird - Large		SALB
XGT	2	Australasian gannet	Morus serrator	DIVE
XGA	2	Great albatrosses	Diomedea spp.	LALB
XWS	1	Wilson's storm petrel	Oceanites oceanicus	SML
XST	1	Storm petrels	Hydrobatidae (Family)	SML
XPV	1	Broad-billed prion	Pachyptila vittata	SML
XPT	1	Pterodroma petrels	Pterodroma spp.	MED
XPS	1	Pied shag	Phalacrocorax varius	DIVE
XPM	1	Mid-sized Petrels & Shearwaters	Pterodroma, Procellaria & Puffinus spp.	MED
XPB	1	Buller's and Pacific albatross	Thalassarche bulleri	SALB
XNR	1	Northern royal albatross	Diomedea sanfordi	LALB
XNB	1	Pacific albatross	Thalassarche bulleri platei	SALB
XIY	1	Indian yellow-nosed albatross	Thalassarche carteri	SALB
XHG	1	Shags	Phalacrocoracidae (Family)	DIVE
XGM	1	Grey-headed albatross	Thalassarche chrysostoma	SALB
XFT	1	Black-bellied storm petrel	Fregetta tropica	SML
XCR	1	Crested penguins	Eudyptes spp.	DIVE

C. CALCULATION OF THE RISK

Our intention was to develop a risk metric based on the probability of a bird capture given management level m, whilst accounting for variability in captures associated with the target fishery, grid, season and other covariates that may affect captures independently of fishing practices. Any particular combination of these (non-management) covariates is referred to using the strata subscript j.

The statistical model proposed allows us to estimate the odds, $\theta_{j,m}$. Using the link function η appropriate for the probability mass function being assumed (Sroka & Nagaraja 2018), we can write the odds as a function of the predictors:

$$\theta_{j,m} = \frac{p_{j,m}}{1-p_{j,m}} = \exp(\mu + \cdots + \beta_m)$$

The probability of capture is:

$$p_{j,m} = \frac{\theta_{j,m}}{1+\theta_{j,m}}$$

We require a method for integrating across j strata to calculate an overall probability of capture, which we refer to as ϕ_m. This can be achieved by either integrating directly across probabilities $p_{j,m}$, or by integrating across the odds and then back calculating the probability (Allard et al. 2012). The latter approach is more convenient, because it allows our risk metric to be related directly to the model coefficients. Taking the geometric mean of the odds, where n_j is the number of strata, we can write:

$$\Theta_m = \left(\prod_j \frac{p_{j,m}}{1-p_{j,m}} \right)^{1/n_j} = \exp(\mu + \beta_m) \tag{18}$$

since the coefficients sum to zero. We can then extract an approximation to the overall probability of capture as a function of μ and β_m:

$$\phi_m \propto \frac{\Theta_m}{1+\Theta_m} = \frac{\exp(\mu+\beta_m)}{1+\exp(\mu+\beta_m)} = R_m \tag{19}$$

which we use as our metric of risk. The β_m coefficients have a prior probability centered on zero, meaning that in the absence of information to update the coefficient value during the model fit, we would expect $\beta_m = 0$. We use this as a reference, i.e. $R_{REF} = \exp(\mu)/(1+\exp(\mu))$; against which to compare estimates of R_m. If $R_m \neq R_{REF}$ then it provides evidence for an effect of management covariate m on the probability of bird capture.

The relationship between ϕ_m and R_m is only approximate (Allard et al. 2012, Satopaa et al. 2014). This can be illustrated using the link functions listed in Table 3. For the Poisson distribution for example, we can calculate a probability of capture as follows:

$$\mu + \beta_m = \eta(\lambda_m)$$

$$\implies \exp(\mu+\beta_m) = \exp(\lambda_m) - 1$$

and therefore:

$$\frac{\exp(\mu+\beta_m)}{1+\exp(\mu+\beta_m)} = 1 - \exp(-\lambda_m)$$

This is the probability of an event according to a Poisson distribution with rate parameter λ_m, which is the rate at the geometric mean of the covariates. This is not the same as the expectation of

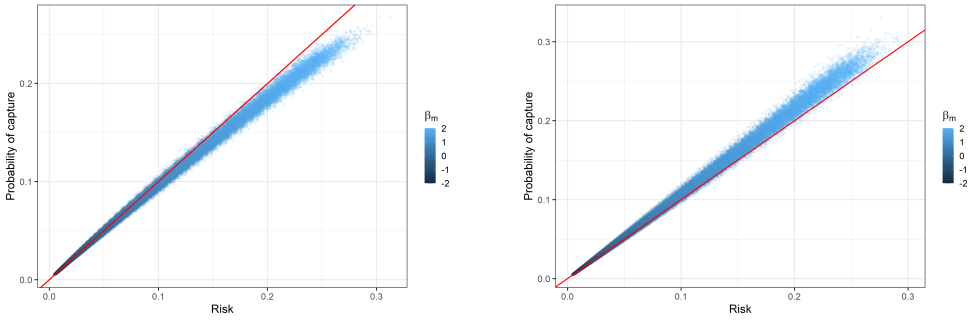

(a) Poisson distribution

(b) Negative binomial distribution

Figure A1: Plot of the risk (Equation 19) against the geometric mean of the probability of a positive capture (Table 3) across all covariate strata j for the Base model. The β_m coefficient was fixed on input.

$1-\exp(-\lambda_{j,m})$ across all covariates, however the approximation is close. Figure A1 illustrates the relationship between the risk, as calculated using Equation 19 and the geometric mean of the estimated probability of a positive capture, taken across all covariate strata in the Base model. The approximation is good for risk values of less than 10% and is therefore suitable for the current application (Table 4). Satopaa et al. (2014) propose an exponent Θ_m^a to make the relationship exact, and we suggest that this would be useful to explore in future work.

We have therefore succeeded in deriving a risk metric that is closely related to the probability of capture and easily calculated directly from covariates estimated during the model fit.

D. CONVERGENCE DIAGNOSTICS

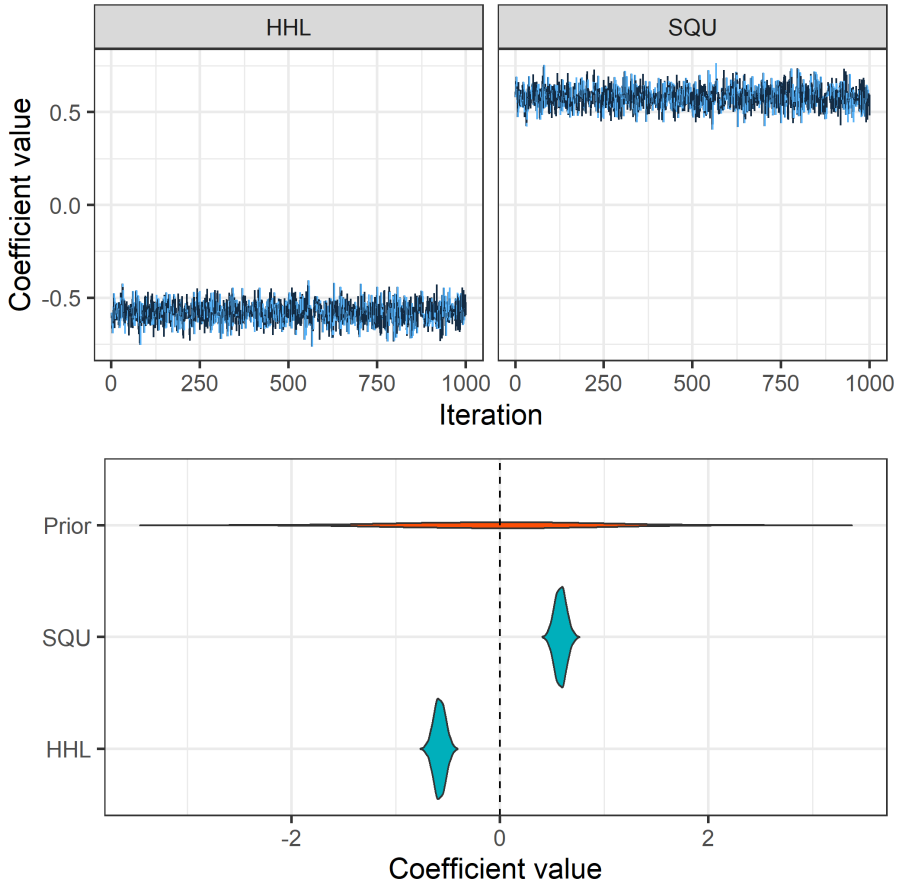

Figure A2: Trace and violin plots showing updates to priors for the target fishery (β_q) coefficients following fit of the Base model.

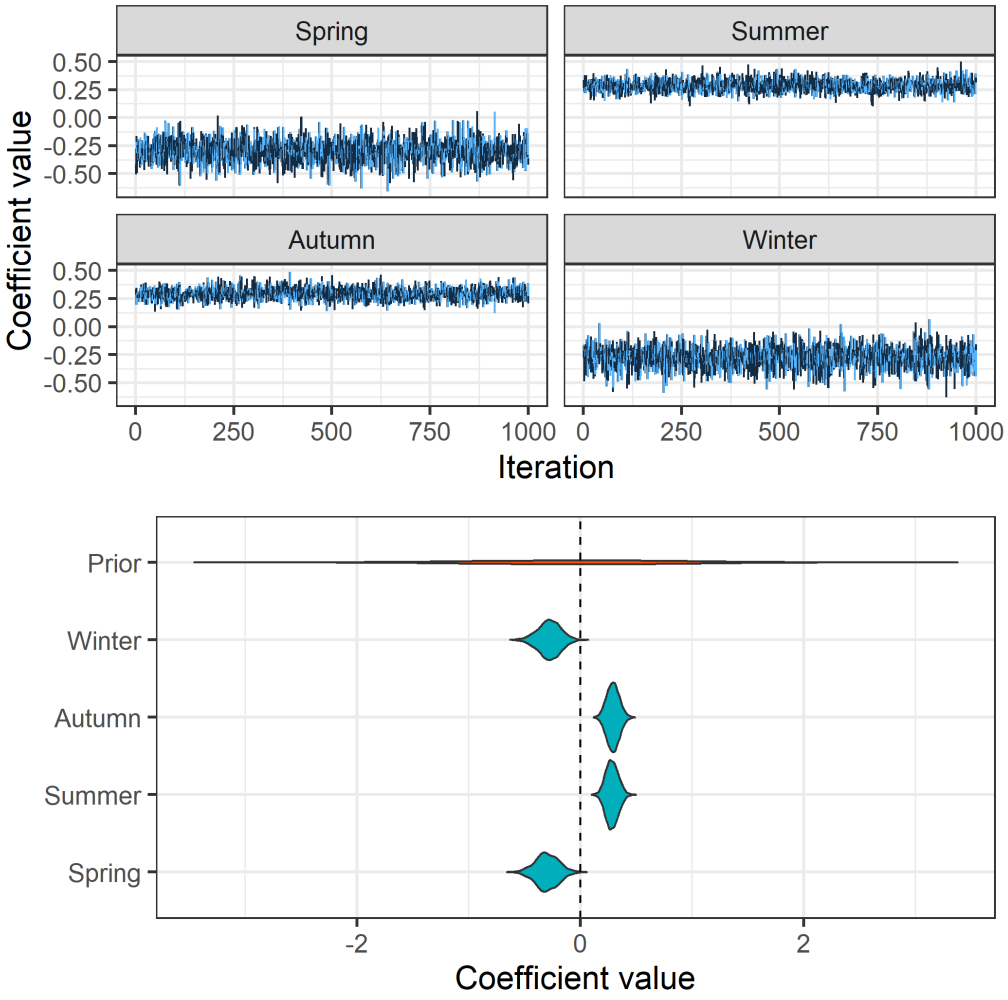

Figure A3: Trace and violin plots showing updates to priors for the season (β_r) coefficients following fit of the Base model.

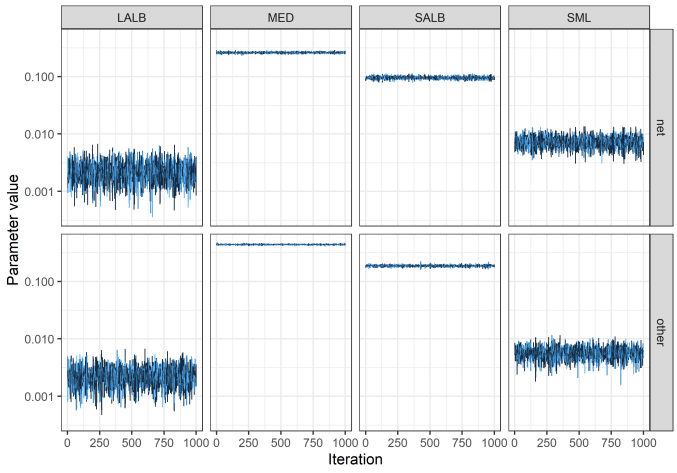

Figure A4: Trace plots for vulnerability parameters following fit of the Base model.

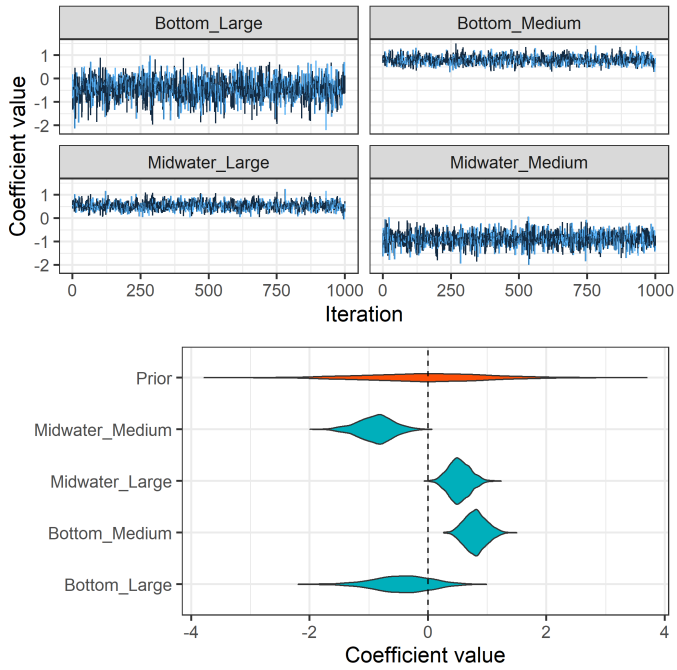

Figure A5: Trace and violin plots showing vessel class coefficient updates for the Base$^+$ model.

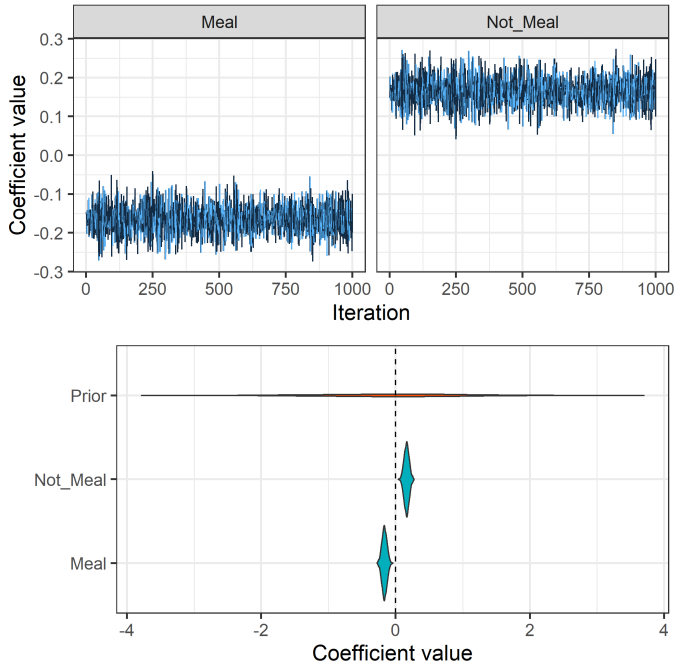

Figure A6: Trace and violin plots showing waste coefficient updates for the Base$^+$ model.

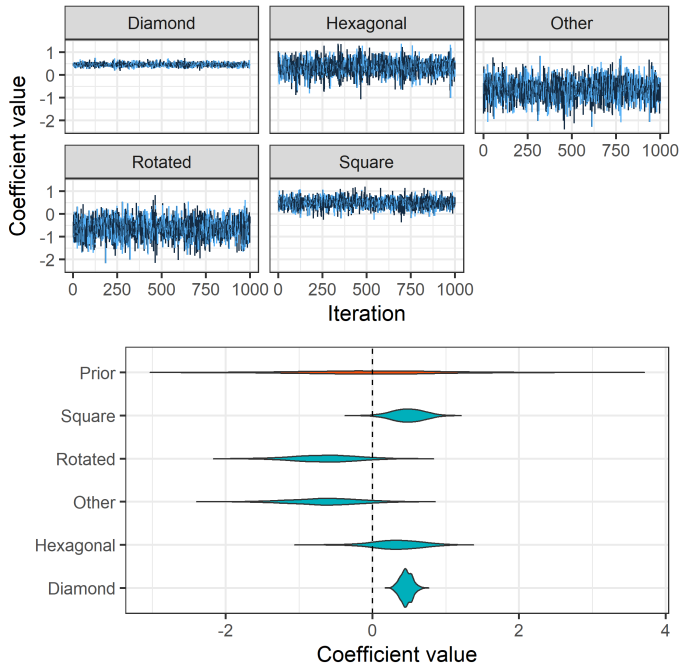

Figure A7: Trace and violin plots showing coefficient updates for the codend net configuration, β_m.

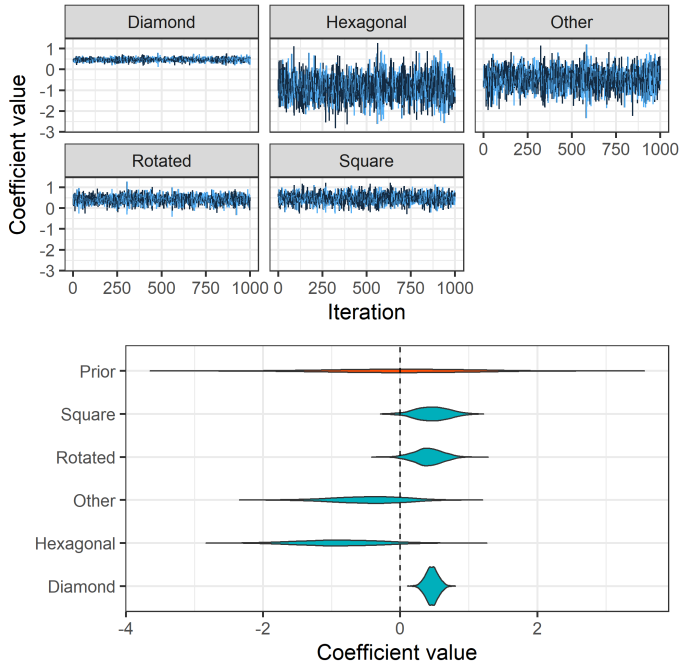

Figure A8: Trace and violin plots showing coefficient updates for lengthener net configuration, β_m.

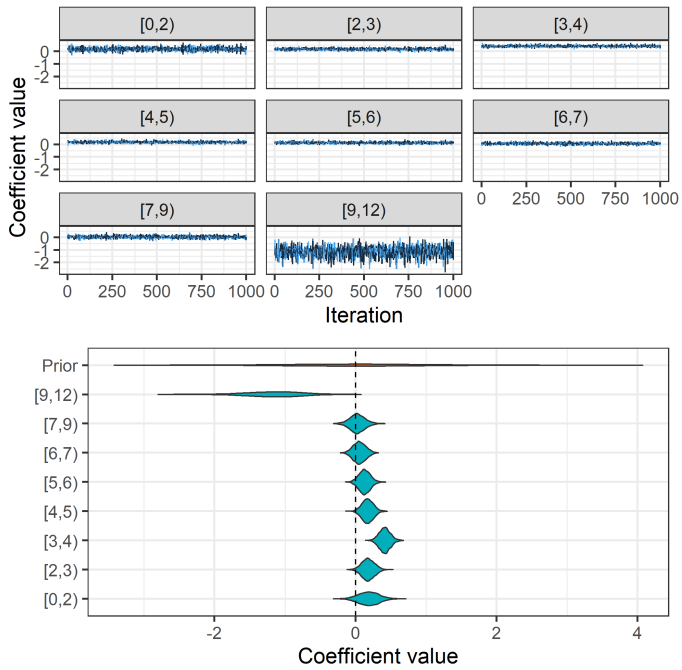

Figure A9: Trace and violin plots showing coefficient updates for the Beaufort scale β_m.

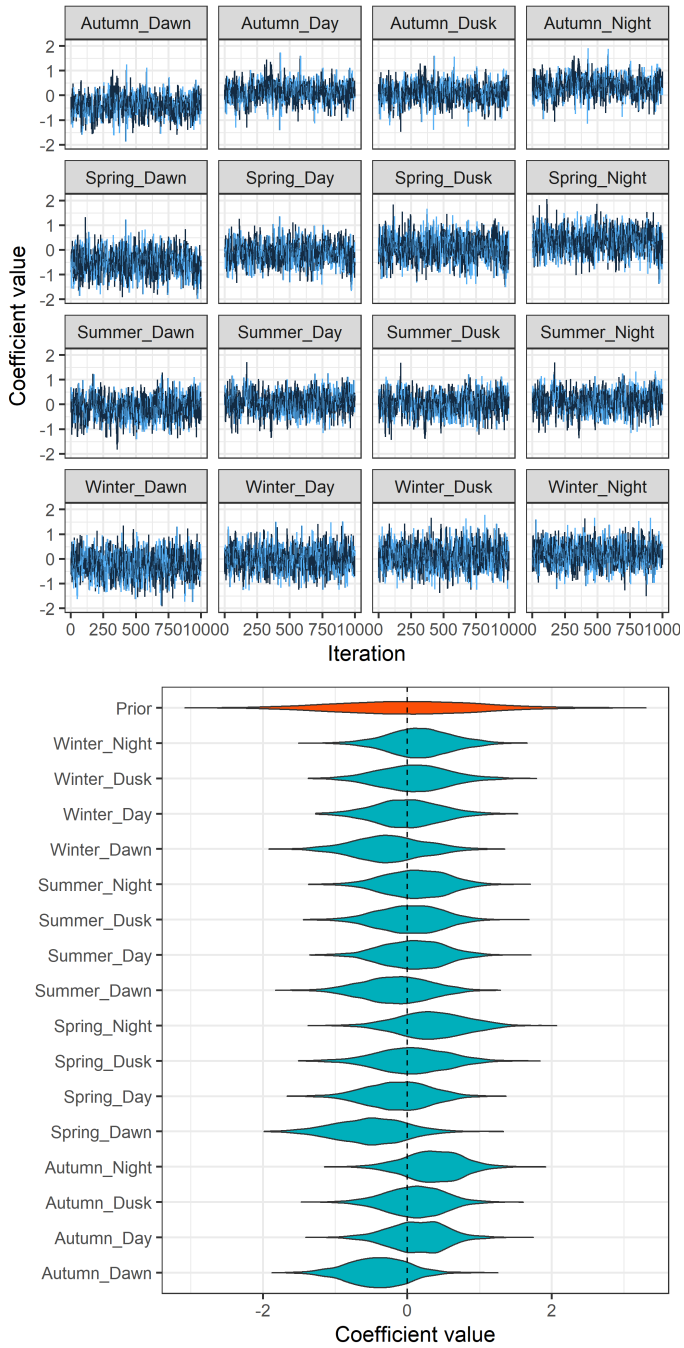

Figure A10: Trace and violin plots showing coefficient updates for the time of haul, β_m.

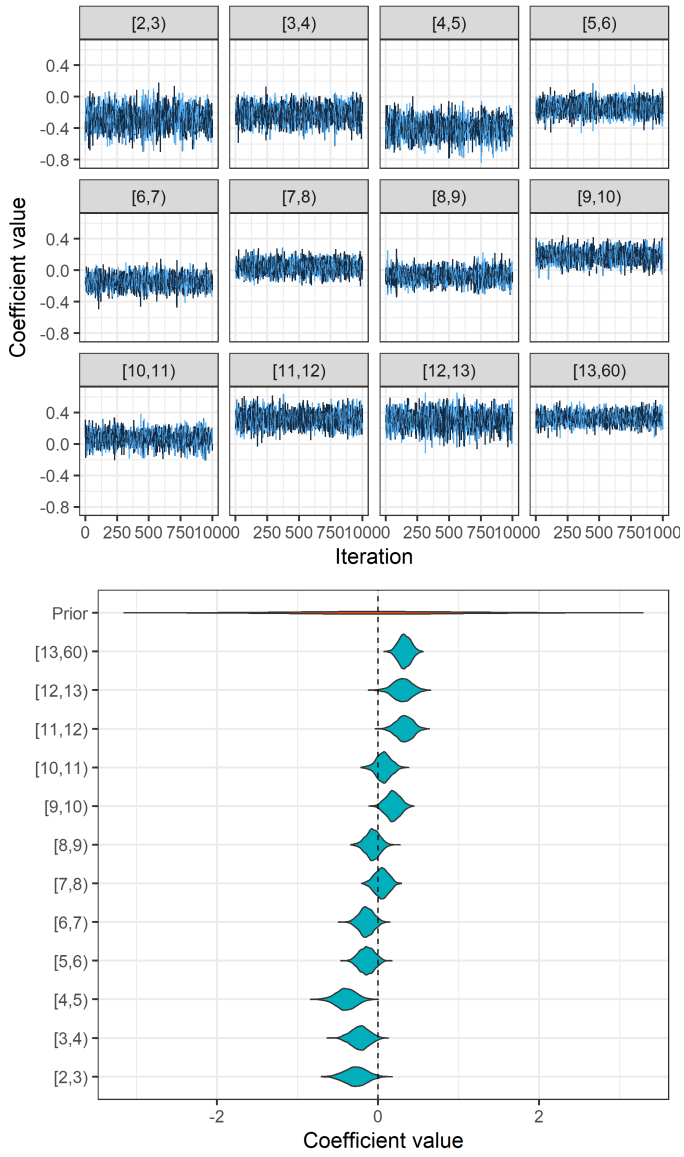

Figure A11: Trace and violin plots showing coefficient updates for the time on surface, β_m.

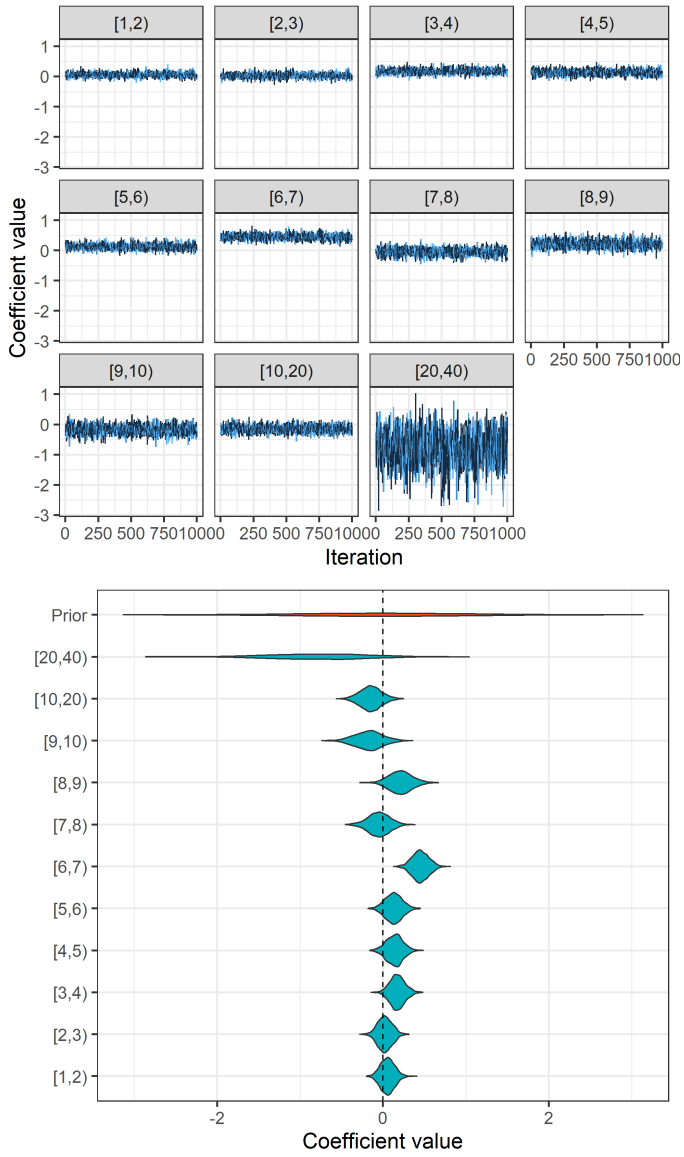

Figure A12: Trace and violin plots showing coefficient updates for the local commercial fishing effort, β_m.

E. MODEL CODE

Code listing A1: Stan code for Poisson model

```
/*
** MULTI-NOMIAL REGRESSION
** ON CAPTURE PROBABILITY
**
*/
functions {

   real inv_link(real x) {

      return log(exp(x) + 1);
   }
}
data {

   // DIMENSIONS
   int N; // RECORDS

   // predictors
   int Q; // FISHERY GROUP
   int G; // GRID
   int R; // SEASON

   // LOOK-UP VECTORS
   int XG[N];
   int XQ[N];
   int XR[N];

   // DATA
   int effort[N]; // OBSERVED EVENTS
   int n[N, 2, 4, 2]; // NUMBERS PER OBSERVATION CATEGORY
}
transformed data {

   // OBSERVATION CATEGORIES
   int C = 2; // CAPTURE TYPE
   int S = 4; // SPECIES GROUP
   int A = 2; // ALIVE/DEAD
}
parameters {

   // Regression
   // parameters
   real mu;
   vector[Q - 1] betaQ_;
   vector[R - 1] betaR_;
   vector[G - 1] betaG_;

   // Conditional
   // Multi-nomial
   // probabilities for
   // captures per
   // capture type,
   // species and status
   simplex[C * S * A] p_mult;
}
transformed parameters {

   real alpha[N];
   real theta[C, S, A];

   // sum-to-zero factor covariates
   vector[Q] betaQ = append_row(betaQ_, -sum(betaQ_));
   vector[R] betaR = append_row(betaR_, -sum(betaR_));
   vector[G] betaG = append_row(betaG_, -sum(betaG_));

   // multi-nomial probabilties
   // [sum to one across species,
   // capture types and alive/dead]
   {
      int l = 1;
      for (i in 1:C) {
         for (j in 1:S) {
            for (k in 1:A) {
               theta[i, j, k] = p_mult[l];
               l += 1;
            }
         }
      }
   }

   // link capture rate
   for (i in 1:N) {

      alpha[i] = mu + betaQ[XQ[i]] + betaG[XG[i]] + betaR[XR[i]];
   }
}
```

```
model {

   // COVARIATES
   betaQ_ ~ std_normal();
   betaG_ ~ std_normal();
   betaR_ ~ std_normal();

   {
      // expected captures
      real lambda;

      for (i in 1:N) {

         // captures for
         // each multi-nomial
         // observation
         for (j in 1:C) {
            for (k in 1:S) {
               for (l in 1:A) {

                  lambda = inv_link(alpha[i]) * effort[i] * theta[j, k, l];

                  // Poisson likelihood
                  n[i, j, k, l] ~ poisson(lambda);
               }
            }
         }
      }
   }
}
generated quantities {

   // reference values
   real pcapture_ref;
   real risk_ref;

   // expected number
   // of captures
   real n_hat[N, C, S, A];

   // expected number
   // of positive capture
   // events
   real n_pos_hat[N, C, S, A];

   for (i in 1:N) {
      for (j in 1:C) {
         for (k in 1:S) {
            for (l in 1:A) {

               n_hat[i, j, k, l] = inv_link(alpha[i]) * effort[i] * theta[j, k, l];

               n_pos_hat[i, j, k, l] = (1.0 - exp(-inv_link(alpha[i]))) * theta[j, k, l] * effort[i];
            }
         }
      }

   }

   // reference risk
   pcapture_ref = 1.0 - exp(-inv_link(mu));
   risk_ref = exp(mu) / (1 + exp(mu));
}
```

Code listing A2: Stan code for Negative Binomial model

```
/*
** MULTI-NOMIAL REGRESSION
** ON CAPTURE PROBABILITY
**
*/
functions {

   real inv_link(real x, real delta) {

      return (pow(exp(x) + 1.0, 1.0 / delta) - 1.0) * delta;
   }
}
data {

   // DIMENSIONS
   int N; // RECORDS

   // predictors
   int Q; // FISHERY GROUP
   int G; // GRID
   int R; // SEASON

   // LOOK-UP VECTORS
   int XG[N];
   int XQ[N];
   int XR[N];

   // DATA
   int effort[N]; // OBSERVED EVENTS
   int n[N, 2, 4, 2]; // NUMBERS PER OBSERVATION CATEGORY
}
transformed data {

   // OBSERVATION CATEGORIES
   int C = 2; // CAPTURE TYPE
   int S = 4; // SPECIES GROUP
   int A = 2; // ALIVE/DEAD
}
parameters {

   // Regression
   // parameters
   real mu;
   vector[Q - 1] betaQ_;
   vector[R - 1] betaR_;
   vector[G - 1] betaG_;

   // Conditional
   // Multi-nomial
   // probabilities for
   // captures per
   // capture type,
   // species and status
   simplex[C * S * A] p_mult;

   // over-dispersion parameter
   real<lower=0> delta_[C * S * A];
}
transformed parameters {

   real alpha[N];
   real theta[C, S, A];
   real delta[C, S, A];

   // sum-to-zero factor covariates
   vector[Q] betaQ = append_row(betaQ_, -sum(betaQ_));
   vector[R] betaR = append_row(betaR_, -sum(betaR_));
   vector[G] betaG = append_row(betaG_, -sum(betaG_));

   // multi-nomial probabilties
   // [sum to one across species,
   // capture types and alive/dead]
   {
      int l = 1;
      for (i in 1:C) {
         for (j in 1:S) {
            for (k in 1:A) {
               theta[i, j, k] = p_mult[l];
               delta[i, j, k] = delta_[l];
               l += 1;
            }
         }
      }
   }

   // link capture rate
   for (i in 1:N) {

      alpha[i] = mu + betaQ[XQ[i]] + betaG[XG[i]] + betaR[XR[i]];
   }
```

```
}
model {

   // COVARIATES
   betaQ_ ~ std_normal();
   betaG_ ~ std_normal();
   betaR_ ~ std_normal();

   {
      // expected captures
      real lambda;

      for (i in 1:N) {

         // captures for
         // each multi-nomial
         // observation
         for (j in 1:C) {
            for (k in 1:S) {
               for (l in 1:A) {

                  lambda = inv_link(alpha[i], delta[j, k, l]) * effort[i] * theta[j, k, l];

                  // NB likelihood
                  n[i, j, k, l] ~ neg_binomial_2(lambda, delta[j, k, l]);
               }
            }
         }
      }
   }

   delta_ ~ std_normal();
}
generated quantities {

   // reference values
   real pcapture_ref;
   real risk_ref;

   // expected number
   // of captures
   real n_hat[N, C, S, A];

   // expected number
   // of positive capture
   // events
   real n_pos_hat[N, C, S, A];

   for (i in 1:N) {
      for (j in 1:C) {
         for (k in 1:S) {
            for (l in 1:A) {

               n_hat[i, j, k, l] = inv_link(alpha[i], delta[j, k, l]) * theta[j, k, l] * effort[i];

               n_pos_hat[i, j, k, l] = (1.0 - pow(delta[j, k, l] / (delta[j, k, l] + inv_link(alpha[i], delta[j, k,
                     l])), delta[j, k, l])) * theta[j, k, l] * effort[i];
            }
         }
      }
   }

   // reference risk
   pcapture_ref = (1.0 - pow(mean(delta_) / (mean(delta_) + inv_link(mu, mean(delta_))), mean(delta_)));
   risk_ref = exp(mu) / (1 + exp(mu));
}
```